MEASURED EFFECTS OF THE VARIOUS COMBINATIONS OF NUCLEAR RADIATION, VACUUM, AND CRYOTEMPERATURES ON ENGINEERING MATERIALS

[2] copy

Quarterly Progress Report

1 March 1963 through 31 May 1963

(NASA CR-50987; FZK-167) OTS: $7.60 ph, $2.42

E.
F.

Prepared
George C. Marshall Space
Huntsville, Alaba

Contract No. NAS8-2450 (Mod. 3)
Request No. TP3-85130 (IF)

2. NUCLEAR AEROSPACE RESEARCH FACILITY

GD/FW REPORT
FZK-167
28 JUNE 1963

GIIIIIIID

NUCLEAR AEROSPACE RESEARCH FACILITY

MEASURED EFFECTS OF THE VARIOUS COMBINATIONS OF NUCLEAR RADIATION, VACUUM, AND CRYOTEMPERATURES ON ENGINEERING MATERIALS

Quarterly Progress Report

1 March 1963 through 31 May 1963

E. E. KERLIN
E. T. SMITH

Prepared for
George C. Marshall Space Flight Center
Huntsville, Alabama

Contract No. NAS8-2450 (Mod. 3)
Request No. TP3-85130 (IF)

GENERAL DYNAMICS | FORT WORTH

This report was prepared by General Dynamics/Fort Worth under Contract No. NAS8-2450, Modification 3, Measured Effects of the Various Combinations of Nuclear Radiation, Vacuum, and Cryotemperatures on Engineering Materials, for the George C. Marshall Space Flight Center of the National Aeronautics and Space Administration. The work was administered under the technical direction of the Propulsion and Vehicle Engineering Division, Engineering Materials Branch of the George C. Marshall Space Flight Center, with Eugene C. McKannan acting as project manager.

SUMMARY

This report covers the work performed during the second quarter of operation under Modification 3 to Contract No. NAS8-2450. Provisions of this modification are for the continuation of a series of tests initiated under the original contract to measure the effects of various combinations of nuclear radiation, high vacuum, and cryotemperature on a select group of nonmetallic spacecraft materials.

During this reporting period the work described below was accomplished.

Radiation-Vacuum Tests

Test samples were prepared and mounted with dosimeters on the irradiation racks; modifications and calibration of the dynamic tensile testers were completed; and functional checkout of the high-vacuum systems was made. During the two weeks of reactor irradiation used in this quarter all of the scheduled static samples for both the air and vacuum environments were irradiated and tested. Two irradiations of both the Low-Force and High-Force Dynamic Tensile Testers were performed. Preliminary analysis of the data indicates that both testers functioned satisfactorily during the tests.

Radiation-Cryotemperature Tests

Test specimens were prepared for 12 of the 16 materials scheduled for testing in the program; rework and checkout of the cryogenic experimental assemblies and associated instrumentation were completed; fabrication of thermal-conductivity

measurement apparatus was started; a flux-mapping irradiation run was made; test specimens were irradiated to the planned low and high doses in ambient-air and to the low dose in liquid nitrogen. Subsequent tensile tests of specimens from the ambient-air irradiation were conducted at room temperature with the use of an Instron machine. Specimens which had been irradiated while submerged in LN_2 were pulled in tension after irradiation while still submerged in LN_2.

Radiation-Vacuum-Cryotemperature Tests

Test materials were selected; the Electrical Tester was designed and constructed; and detailed design was started on the Mechanical Tester.

TABLE OF CONTENTS

LIST OF FIGURES

LIST OF FIGURES (Cont'd)

LIST OF TABLES

I. INTRODUCTION

Many of the component parts of nuclear-powered spacecraft will be exposed, during flight, to environments composed of the various combinations of nuclear radiation, high vacuum, and cryo-temperatures. The first known tests to measure the engineering properties of nuclear radiation and high vacuum and of nuclear radiation and cryotemperatures were conducted by the Nuclear Aerospace Research Facility at General Dynamics/Fort Worth during 1962. Annual progress reports covering the work have been published (Refs. 1, 2).

The effort during 1963 (outlined and described in Modification 3 to the original contract) is a continuation of that work which was started last year and includes an additional phase of work designed to demonstrate the effects on materials of the triple environment of nuclear radiation, high vacuum, and cryo-temperature. The work performed during the first quarter of 1963 is described in the previous quarterly progress report (Ref. 3). The work performed during the second quarter is reported in this document.

Material categories covered in tests performed during the first year included adhesives, seals, thermal insulations, electrical insulations, structural laminates, thermal-control coatings, potting compounds, and lubricants. Representative tests were those suitable for measuring la-shear strength, ultimate tensile strength, ultimate elongation, stress-strain characterisitcs, weight loss, lubricity, compressive strength and spectral reflectivity.

During the second year's work, essentially the same tests are being performed on a new group of materials selected from the same material categories. Additional tests include the measurement of thermal conductivity, dissipation factor, dielectric strength, T-peel strength, and potted-wire pull-out strength. The thermal-control-coating test has been deleted.

II. COMBINED EFFECTS OF RADIATION AND VACUUM

2.1 Irradiation Tests

During this quarter, two of the four reactor irradiation periods scheduled in the contract for this year were successfully used. The mechanical properties of materials were determined in air after irradiation in air, and in vacuum and air after irradiation in vacuum. Specially built dynamic testers determined the properties of some materials immediately after irradiation while the specimens were still in the vacuum environment. The materials so tested included one or two from each of the following categories: adhesives, laminates, seals, thermal insulations, and electric insulations.

2.1.1 Materials Irradiated

Table 2.1 of the first Quarterly Progress Report (Ref. 3) identifies 50 materials selected for testing in this program. Tables 2.3 through 2.9 from the same report give a complete description of the test parameters and type of data resulting from these tests.

Table 2.1 of this report presents a list of the materials irradiated and tested during the current quarter. The ASTM test specifications used in these tests are described in Table 2.1 of Reference 3. Three of the selected materials were supplied from the vendor after the irradiations had begun. These materials, supplied by Precision Rubber Products, were O-ring compounds PRP 19007, PRP 737-70, PRP 2277. However, a portion of the required data have been obtained; the rest will be obtained if additional reactor space becomes available.

Table 2.1

Nominal Gamma Radiation Doses to Test Specimens Used in Vacuum-Irradiation Tests
[ergs/gm(C)]

Category	Trade Name	Manufacturer	Vacuum Irradiation		Air Irradiation
			Tested In Vacuum	Tested In Air	Tested In Air
Structural Adhesives	Shell 929	Shell Chemical Co.		5(9),1(10),3(10)	5(9),1(10),3(10)
	Shell 934	Shell Chemical Co.		5(9),1(10),3(10)	5(9),1(10),3(10)
	FM-1000	Bloomingdale Rubber Co.		3(10)	1(10),3(10)
	HT-424	Bloomingdale Rubber Co.		5(9),1(10),3(10)	5(9),1(10),3(10)
	Aerobond 430	Adhesive Engr. Co.		5(9),1(10),3(10)	5(9),1(10),3(10)
	Narmco A	Narmco Material Division		5(9),1(10),3(10)	5(9),1(10),3(10)
	FM-47	Bloomingdale Rubber Co.		5(9),1(10),3(10)	5(9),1(10),3(10)
	Metlbond 4021	Narmco Material Division	1(10),3(10)	5(9),1(10),3(10)	5(9),1(10),3(10)
	APCO 1252	Applied Plastics Co.	1(10),3(10)	5(9),1(10),3(10)	5(9),1(10),3(10)
	Narmco C	Narmco Material Division		5(9),1(10),3(10)	5(9),1(10),3(10)

Table 2.1 (Cont'd)

Category	Trade Name	Manufacturer	Vacuum Irradiation		Air Irradiation
			Tested In Vacuum	Tested In Air	Tested In Air
Structural Laminate	Mobiloy 81-AH7	Cordo Moulding Products	1(10),3(10)	5(9),1(10),3(10)	5(9),1(10),3(10)
	Paraplex P-43	Rohm and Haas		5(9),1(10),3(10)	5(9),1(10),3(10)
	DC-2104	Dow Corning Corp.	1(10)	5(9),1(10),3(10)	5(9),1(10),3(10)
	Selectron 5003	Pittsburgh Plate Glass	3(10)	5(9),1(10),3(10)	5(9),1(10),3(10)
	HRP Honeycomb	Applied Plastics Co.		5(9),1(10),3(10)	5(9),1(10),3(10)
Potting Compounds	RTV-60	General Electric		5(9)	5(9)
	RTV-501	Dow Corning Corp.		1(8),5(8),1(9)	1(8),1(9)
	Durock D-133	Physical Science Corp.		3(10)	3(10)
	Scotchcast 212	Minnesota Mining Manufacturing Co.		5(8),1(9),5(9), 3(10)	5(9),3(10)
	EC-2273	Minnesota Mining Manufacturing Co.		1(8),1(9),5(9)	1(8),1(9),5(9)
Electrical Insulation	DC-7-170	Dow Corning Corp.		1(8),5(8),1(9)	1(8),1(9)
	KEL-F-81	Minnesota Mining Manufacturing Co.	1(8),5(8)	5(7),1(8),5(8)	5(7),1(8),5(8)
	Mylar A	E. I. du Pont de Nemours Co.		5(8),5(9),1(10)	5(8),1(10)

Table 2.1 (Cont'd)

Category	Trade Name	Manufacturer	Vacuum Irradiation		Air Irradiation
			Tested In Vacuum	Tested In Air	Tested In Air
Electrical Insulation (cont'd)	Mylar C	E. I. du Pont de Nemours Co.		5(8),1(9),5(9)	5(8),5(9)
	Geon 2046	B. F. Goodrich Chemical Co.		5(8),1(10)	5(8),5(9),1(10)
	Geon 8800	B. F. Goodrich Chemical Co.		5(8),1(10)	5(8),5(9),1(10)
	Estane 5740X1	B. F. Goodrich Chemical Co.		1(9),1(10),3(10)	1(9),1(10),5(10)
	Duroid 5600	Rogers Corp.		1(8),5(8),1(9)	1(8),5(8),1(9)
	Kyner	Pennsalt Chemical Co.		5(7),1(8),1(9)	5(7),1(8)
Dielectric Materials	Marlex	Phillips Chemical Co.		1(8),5(8),1(9)	1(8),1(9)
	Teflon TFE (10 mil)	E. I. du Pont de Nemours Co.	1(8),5(8)	5(7),1(8),5(8)	5(7),1(8),5(8)
	Teflon TFE (40 mil)	E. I. du Pont de Nemours Co.		1(8),5(8)	1(8),5(8)
	Teflon FEP (10 mil)	E. I. du Pont de Nemours Co.		5(7),1(8),5(8)	5(7),5(8)
	Teflon FEP (40 mils)	E. I. du Pont de Nemours Co.		1(8),5(8)	1(8),5(8)

Table 2.1 (Cont'd)

Category	Trade Name	Manufacturer	Vacuum Irradiation		Air Irradiation
			Tested In Vacuum	Tested In Air	Tested In Air
Dielectric Materials (cont'd)	Tedlar	E. I. du Pont de Nemours Co.		1(8),5(8),1(9)	1(8),1(9)
	H-Film	E. I. du Pont de Nemours Co.		1(10),3(10)	5(9),3(10)
	Thermofit	Raytherm Corp.		1(8),1(9),1(10)	1(8),1(9),1(10)
Thermal Insulation	CPR-20	Chemical Plastic Research	1(8),5(8)	5(7),1(8),1(9)	5(7)
	CPR-1021-2	Chemical Plastic Research	5(8)	1(8),5(8)	5(8)
Seals	RA-33860	Marshall Space Flight Center		5(8),1(9),5(9)	5(8),5(9)
	PRP-19007	Precision Rubber Products		5(8),1(9)	
	PRP-737-70-FLX	Precision Rubber Products		5(8),1(9)	
	PRP-2277	Precision Rubber Products	1(8),5(8)	1(8),5(8),1(9)	1(8),1(9)
	66-581	Parker Seal Co.	1(8),5(8)	5(7),1(8),5(8) 1(9)	1(8),1(9)

Two of the formulations to be tested as wire-pull samples (Ref. 3) were not irradiated because of problems in preparing the test specimens.

Reduction and analysis of the raw data is in progress, but because of the small percentage of data that is in final form, the results of the static and dynamic tests will be presented in the third Quarterly Progress Report, to be issued September 1.

2.1.2 Test Equipment

The vacuum-irradiation chambers used this year are the same as those used last year. A detailed description of the systems, vacuum capabilities, and nuclear-spectrum measurements is given in the annual report (Ref. 1). The vacuum systems functioned satisfactorily in all but one of the vacuum irradiations. During this irradiation, one of the thermal over-temperature safety switches shut off one diffusion pump. The pressure slowly climbed to one micron before the end of the irradiation. The pressure during the static vacuum irradiations was between 1×10^{-7} torr and 4×10^{-7} torr.

Two irradiations each of the specimens in the Low-Force Tensile Tester and High-Force Tensile Tester (Ref. 1) were made during this quarter. The lowest pressure during the irradiations was 1.2×10^{-7} torr, while the highest was 3×10^{-6} torr. The dynamic equipment functioned according to design, and data reduction is in progress.

2.2 Future Irradiation Tests

The one remaining test to be conducted this year to evaluate the combined effects of radiation and vacuum is the Bearing Lubricant Test. This test is progressing as planned, with irradiation scheduled to take place during the last week of July.

The Bearing Tester used last year has been modified to incorporate larger R-112 Kearfott servomotors (Ref. 3), two additional test motors to bring the number of test motors to 10, larger flywheels, and provision for cooling water to lower the temperature of the test-lubricant bearings during irradiation.

The lubricants are being applied to the test R3 size bearing by Miniature Precision Bearing Co. and Midwest Research Institute. Miniature Precision Co. is also dynamically balancing the flywheels and determining the control values of the test motors and bearing.

III. COMBINED EFFECTS OF RADIATION AND CRYOTEMPERATURES

3.1 Test-Specimen Preparation

All materials scheduled for testing under Modification 3 to the contract were selected and ordered from sources of supply during the first quarter of operation in 1963. Most of these were received at GD/FW during the month of March, 1963. Work on specimen preparation was started during the first two weeks of April and is described below. Complete specimen descriptions are shown in the previous quarterly progress report (Ref. 3).

Adhesives

Materials A and B. Six-in.-wide, 1/16-in.-thick aluminum adherent sheets were furnished to the George C. Marshall Space Flight Center (MSFC) where Material A (AF-40, Minn. Mining and Mfg. Co.) was applied in lap-shear form. One-in.-wide specimens were then milled at GD/FW. Lap-shear specimens for Material B (Aerobond 422J, Adhesives Engineering Co.) were obtained from an earlier test at GD/FW.

Seals

Materials C and D. O-rings manufactured from Material C (Viton B, Precision Rubber Co.) were not received in time to be included in the first irradiation tests. Material D (Polymer SP, E. I. du Pont) was milled into dumbbell-type specimens with a 1/2- by 1/8-in. cross-sectional area in the center section. Aluminum doublers were glued to the 1-1/4-in.-wide end sections with Epon 934 made by Shell Chemical Company.

Thermal Insulations

Materials E, F, and G. The component parts for the thermal-insulation foams, Material E (Stafoam AA-402, American Latex Products) and Materials F and G (CPR-20 and CPR-1021, Chemical Plastics Research Co.), were received in March, but the materials are not scheduled for foaming into place in the thermal-conductivity testers until the first week of June.

Electrical Insulations

Materials H, I, and J. Specimens from Materials H and I (Geon 8800 with polyester plasticizer, B. F. Goodrich Co.; Duroid 5600, Rogers Corp.) were made identical to those for Material D, and are scheduled for tensile tests. Material J (Milimene-Glass 6038, Minn. Mining and Mfg. Co.) was made into dumbbell-type specimens with a 1/4- by 1/8-in. cross-sectional area in the narrowed section of the specimen and a 1-1/4-in. width on the ends. Aluminum doublers were glued to both sides of each end.

Structural Laminates

Materials K and L. These materials (CTL-91-LD, Eldon Fiber-Glass Mg. Co.; DC-2104 with glass fabric, Dow Corning Mfg. Co.) were made into dumbbell specimens like those of Material J.

Potting Compounds

Materials M and N. Standard electrical hook-up wire was potted in Material M (Epon 828/Z, Shell Chemical Co.) by GD/FW and in Material N (EC-2273 B/A, Minn. Mining and Mfg. Co.) by the manufacturer's test laboratories. The potting operation was successful for both materials.

Sealants

Materials O and P. These materials (EC-1949 and EC-1663, Minn. Mining and Mfg. Co.) were applied, according to the manufacturer's recommendations, to 6-in.-wide adherent sheets. The T-peel specimens were then cut and formed from these sheets in accordance with the design shown in Reference 3.

Only enough specimens for the ambient-air and low-dose LN_2 irradiations were made at first, so that any testing problems that might arise as a result of specimen shapes or sizes, doubler application, or slot drillings could be corrected for specimens used in succeeding tests. This approach proved to be advantageous, in that several discrepancies did occur in the original tests. For instance, an error in drilling dimensions for the longer dumbbell specimens caused the bottom of the specimens to rub on the base of the lower clevis assembly. A satisfactory fit will result

after subsequent specimens shortened by approximately 1/8 in.

Another problem was encountered with specimens from Materials D and H, i.e., plastics that were machined into the shorter of the two dumbbell shapes (1/2- by 1/8-in. cross-sectional area in the necked-down portion of the specimen). When tested for ultimate tensile strength, most of the specimens broke in the doubler section rather than in the narrowed section. Reasons for this have not been definitely established at this time. Possibilities include the (1) effects of different thermal-expansion coefficients for the test material and the aluminum doublers and (2) chemical reactions between the test material and the doubler adhesive. For the remaining tests, specimens from these two materials will be modified by reducing the center cross-sectional area by one-half. This should ensure that breaks during tensile tests will occur in the narrowed section. In addition, force-to-break should still be sufficiently high at cryotemperatures to provide good data.

3.2 Experimental-Assembly Rework and Calibration

Re-use of the experimental assemblies after previous tests generally involves a complete decontamination and overhaul. After radioactivity of the systems has decayed to safe levels, the upper structure and cryogen chamber (dewar) are thoroughly scrubbed and steam-cleaned to remove all loose radioactive contamination. Both sections are then reassembled in the Irradiated Materials Laboratory (IML). The slave cylinders are filled with new hydraulic fluid, checked for satisfactory operation, and capped off. All Teflon shaft seals are replaced with new ones, new

dewar gaskets are installed, and the shaft-seal riser heaters are checked for proper operation. LVDT's, drive motors, and associated wiring are checked for radiation damage, electrical shorts or open circuits, and proper operation. The Refrasil insulation in the outer chamber of the dewar is removed, and the inner LN_2 chamber is inspected for breaks. The vacuum chamber in the dewar is then checked and pulled to approximately 10 microns pressure.

After the April 22nd irradiation tests this year, inspection of the west dewar revealed that the walls to the main cryogen chamber were ruptured at the welds around the bottom (see Fig. 3.1). An investigation was initiated immediately to determine what had taken place and why.

Since nothing of an unusual nature had occurred during the tests, a check was made of the cryogen-chamber pressure-transducer recorder chart for the period during postirradiation warm-up. Six pressure pips, spaced approximately 10 min apart, were found to be recorded on the chart about 6-8 hr after shutdown of both the reactor and LN_2 flow. This happens to be the approximately time required to boil off a 16-gal chamber of LN_2. It was also ascertained that personnel in the reactor area had heard a sound resembling a muffled explosion at about the time the pressure pips were recorded.

At this point in the investigation, a series of detonations took place in two LN_2 dewars being irradiated in a separate experiment. Associated with these detonations was a very strong odor of

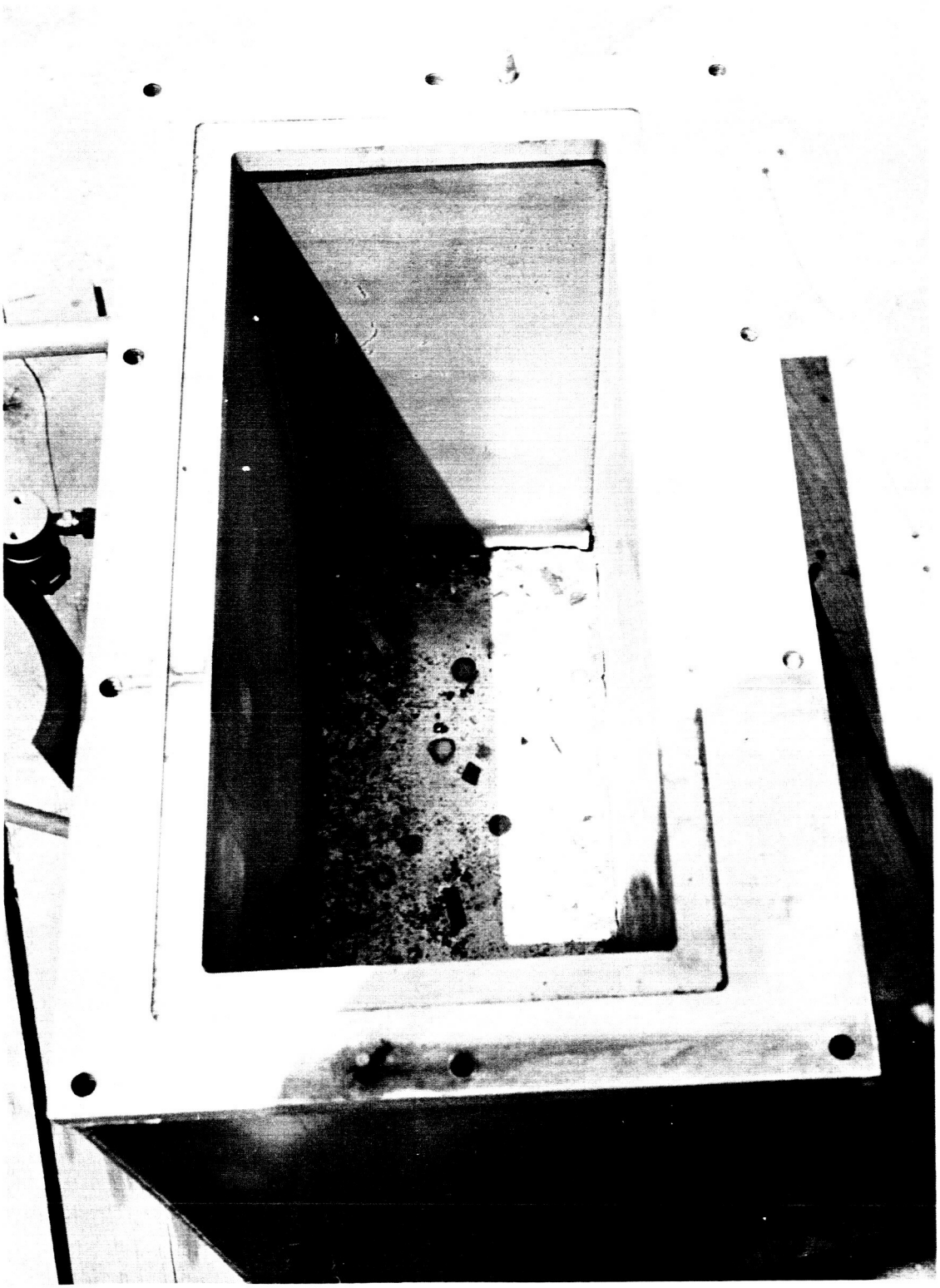

Figure 3.1 Experimental-Assembly Dewar with Ruptured Inner Wall

ozone near the dewars. From this it was theorized that highly exothermic ozone-to-oxygen disassociation reactions were taking place in the dewars during the final warmup period.

It is common knowledge that ozone is formed by irradiation of oxygen, and reference to the boiling point of LOX and LN_2 revealed that LOX impurities in continuously supplied boiling LN_2 would build up in concentration. A check of the sources of supply for LN_2 delivered to NARF during the past year showed that those sources used last year (when several LN_2 irradiations were carried out without incident) had supplied LN_2 with a guaranteed LOX content of less than 20 ppm.

On the other hand, the LN_2 used this year (for the irradiation tests involving the detonations described above) all came from a source which furnished tank analyses showing an LN_2 purity of 99.8%. The possibility that the remaining 0.2% could be mostly LOX thus indicates that, in the process of boiling off as much as 1000 gal of LN_2, the LOX content in the dewar could gradually build up to a total of approximately 5 to 10 gal. With this amount of oxygen being transformed into ozone, resultant disassociation reactions could very well be severe.

A literature survey conducted along with the above investigation revealed that liquid ozone can indeed detonate with the presence of even the slightest amount of organic or other types of sensitizers. Several papers uncovered during the investigation described explosions that had occurred in irradiated LN_2 dewars at various installations throughout the country (Refs. 4, 5).

As a result of the above investigation, it has been concluded that LN_2 irradiation tests in which the experimental assemblies are used can be conducted safely and without detonations by using LN_2 containing less than 20 ppm.

During the course of repair of the ruptured dewar, a decision was made to conduct, during the next LN_2 irradiation test, a parallel experiment to measure the effectiveness of cold nitrogen gas as an insulation against heat flow from the outer walls of the dewar to the LN_2. Vacuum insulation will not be used. Instead, 1/4-in.-diam holes will be drilled on 2-in. centers around the top edge of the cryogen chamber. Additional holes will be drilled in the bottom of the outer vacuum chamber wall. These will allow evaporated cryogen to flow into the vacuum chamber at the top, down around the sides, out of the vacuum chamber and into the next chamber at the bottom, up the sides of this chamber, and out to the atmosphere through the 1-in. outlet port. An attempt will be made to measure the difference in LN_2-consumption rates for this system against one using a vacuum next to the cryogen chamber.

Recalibration of ten LVDT's and five dynamometers on the west experimental assembly preceded the first LN_2 irradiation. This work is required as a part of every test to ensure maximum accuracy in the data. Generally, a new set of 120-ft-long electrical harness for the assemblies must be made up for each successive run. This is because of the high radioactivity resulting in the assembly ends of the hardness and the usual rough treatment they receive during a test.

3.3 Thermal-Conductivity Test Apparatus

Fabrication of parts for the thermal-conductivity test apparatus is approximately 75% complete at this time. All instrumentation for the tests has been assembled and is shown in Figure 3.2. As can be noted, the equipment consists of (1) a GD/FW-built heater control panel for individual control of two guard heaters and one test heater on each of three testers, (2) a GD/FW-built thermocouple control panel for individual selection of any one of 36 thermocouples, (3) a GD/FW-built voltage selector panel for individual selection of the various voltage and current values for readout on a digital voltmeter, (4) a Non-Linear Systems, Inc., Model V-35 digital voltmeter, (5) a Kintel Model 191A amplifier, (6) a Non-Linear Systems, Inc., Model 125C converter, (7) a Rubicon potentiometer, and (8) a Mid-Eastern Electronics Model ST60-6 dc power supply.

For operational checkout of the entire test, one pilot-model tester will be assembled. This work is in progress at the present time. Checkout of the unit will consist of application of controlled amounts of heat to the test and guard heaters, establishment of steady-state temperature conditions at the twelve thermocouple locations, and calculation of the thermal conductivity from equations shown in Reference 3. This procedure will be followed with the tester at room temperature and also with it submerged in LN_2. The coefficient of thermal conductivity will be determined for the thermal insulation foam Stafoam AA-402.

NPC 17,782
31-7139

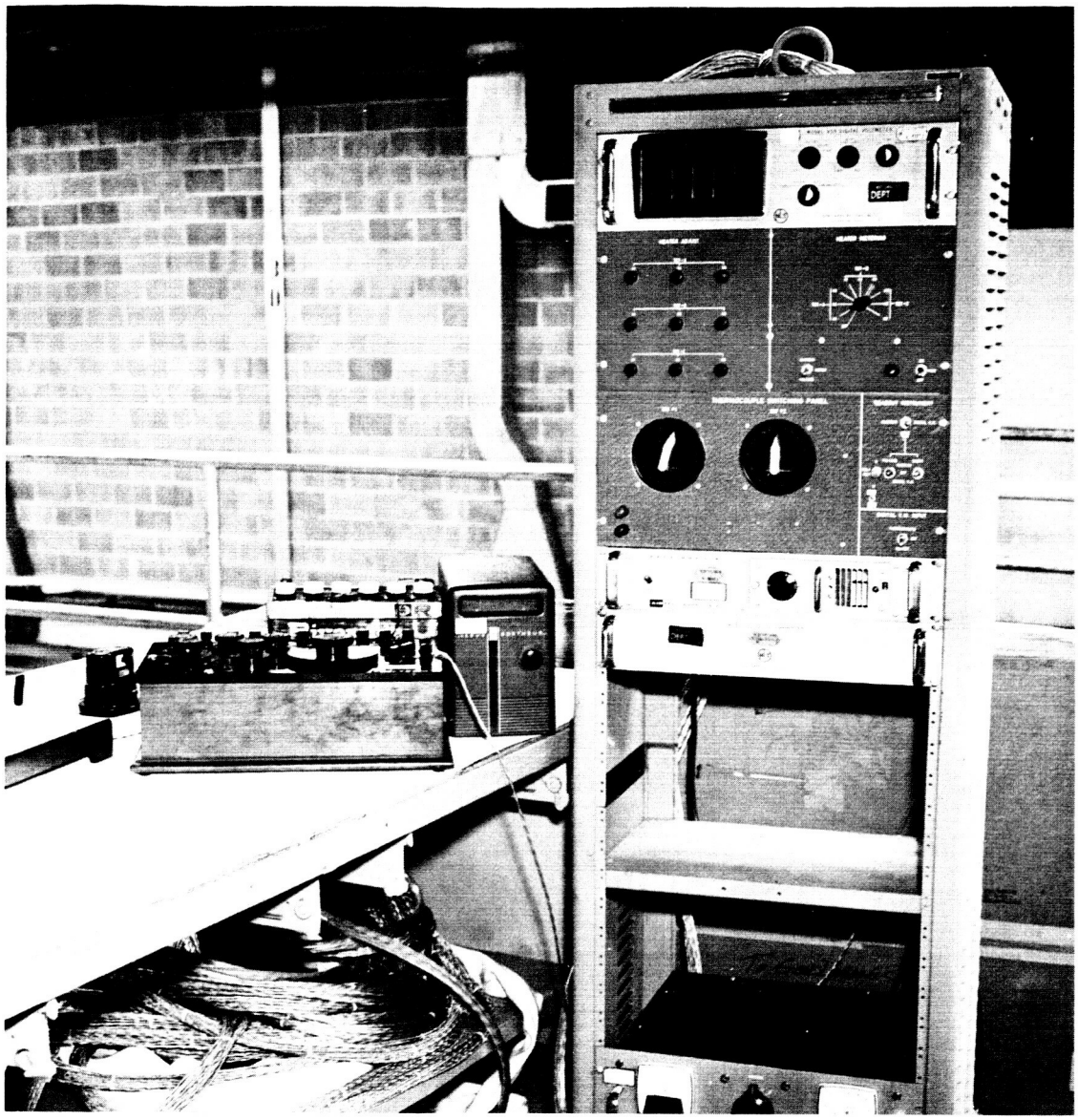

Figure 3.2 Thermal-Conductivity Test Instrumentation

3.4 Mapping Irradiation

The neutron fluxes and gamma dose rates in air at centerline and ± 10 in. off centerline have been well established for the east, west, and north irradiation positions of the Ground Test Reactor (GTR) at NARF (Ref. 6). These values are plotted in Figures 3.3 through 3.14. It should be noted that these data are established for a 4-in. thickness of water between the core and the north irradiation position and for a 4.25-in. thickness of water between the core and the east and west positions.

These data are successfully used in predicting doses for specimens irradiated in air at the three positions, but variations in established dose rates occur when metallic or organic structure is placed between the reactor core and the specimens being irradiated. Calculations can be made for these variations if the interposed material is uniform in shape, size, and density but for other arrangements, a pre-test mapping irradiation is desirable.

It was decided this year that a mapping run for the NASA cryogenic experimental assemblies would be beneficial in predicting dose rates for specimens located below each of the ten pull rods. The plan involved operation of the reactor for two 1-hr runs at power level of 1 Mw. During the first run, the east and north experimental assemblies were mapped.

Dosimetry was mounted to the lower box frames of the assemblies. As can be seen in Figure 3.15, a complete dosimetry packet was located at the exact sample position for pull rods 1, 3, 5,

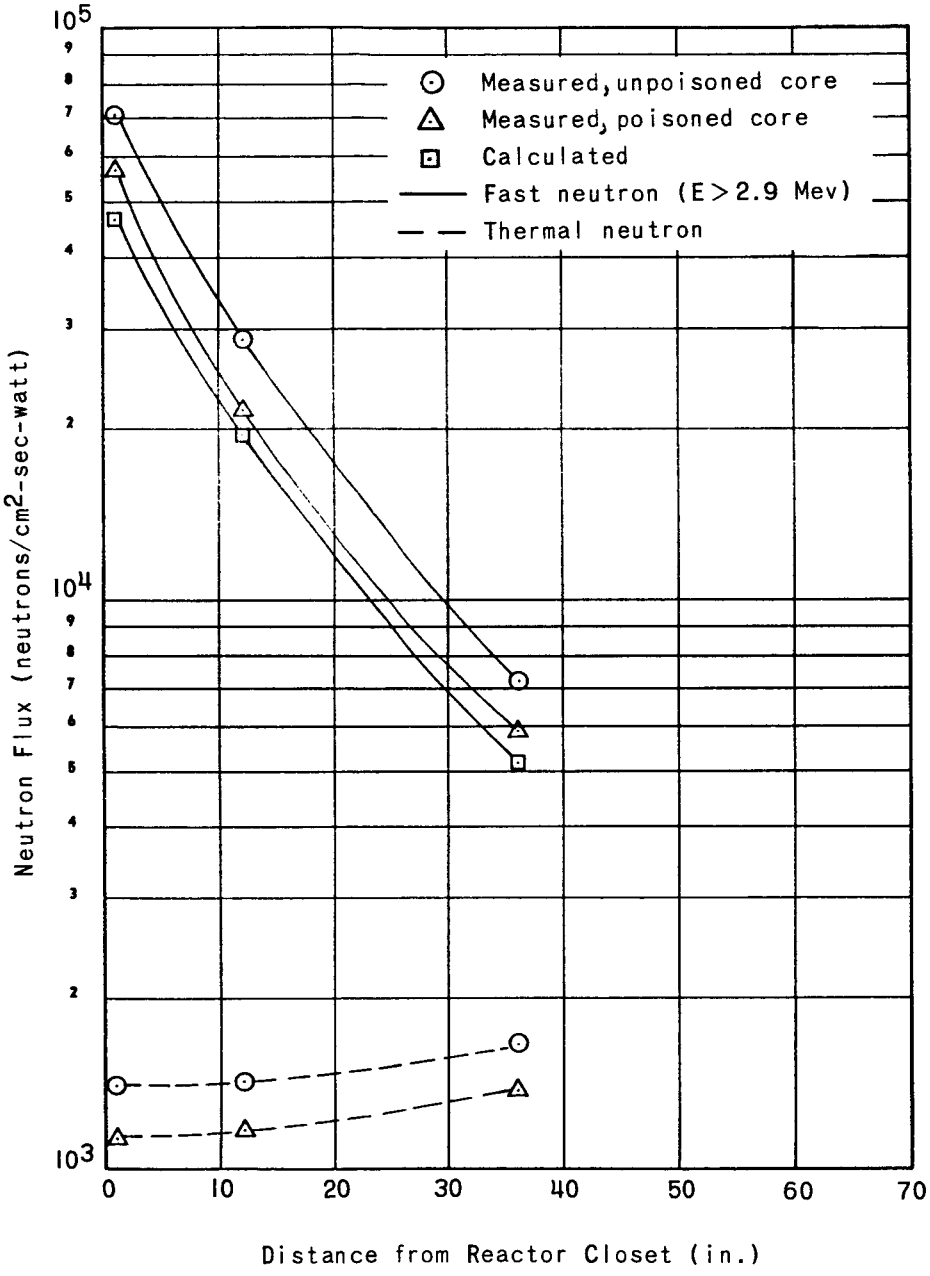

Figure 3.3 Average Neutron Flux on Rack Centerline: North Face

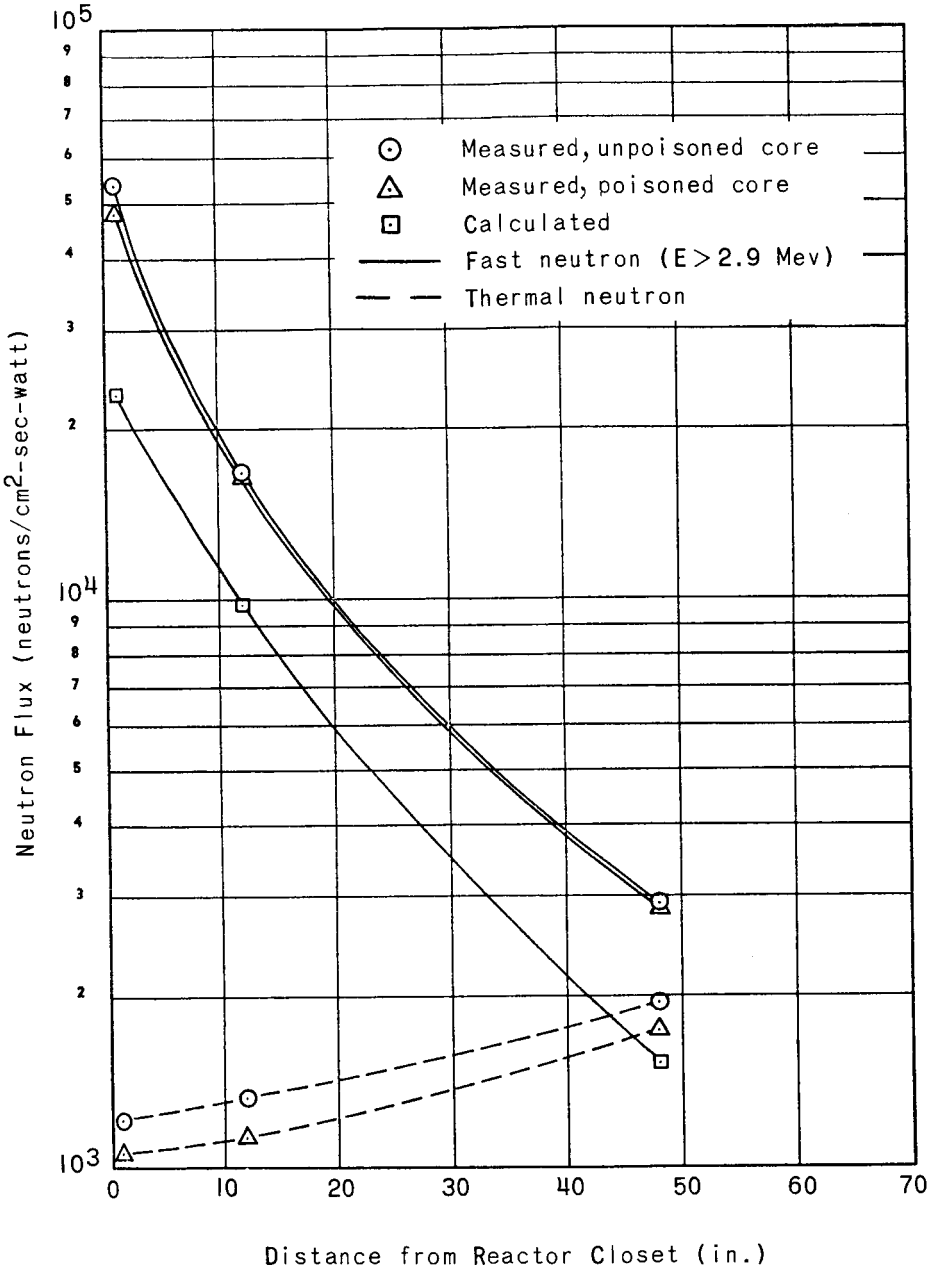

Figure 3.4 Average Neutron Flux on Rack Centerline: East Face

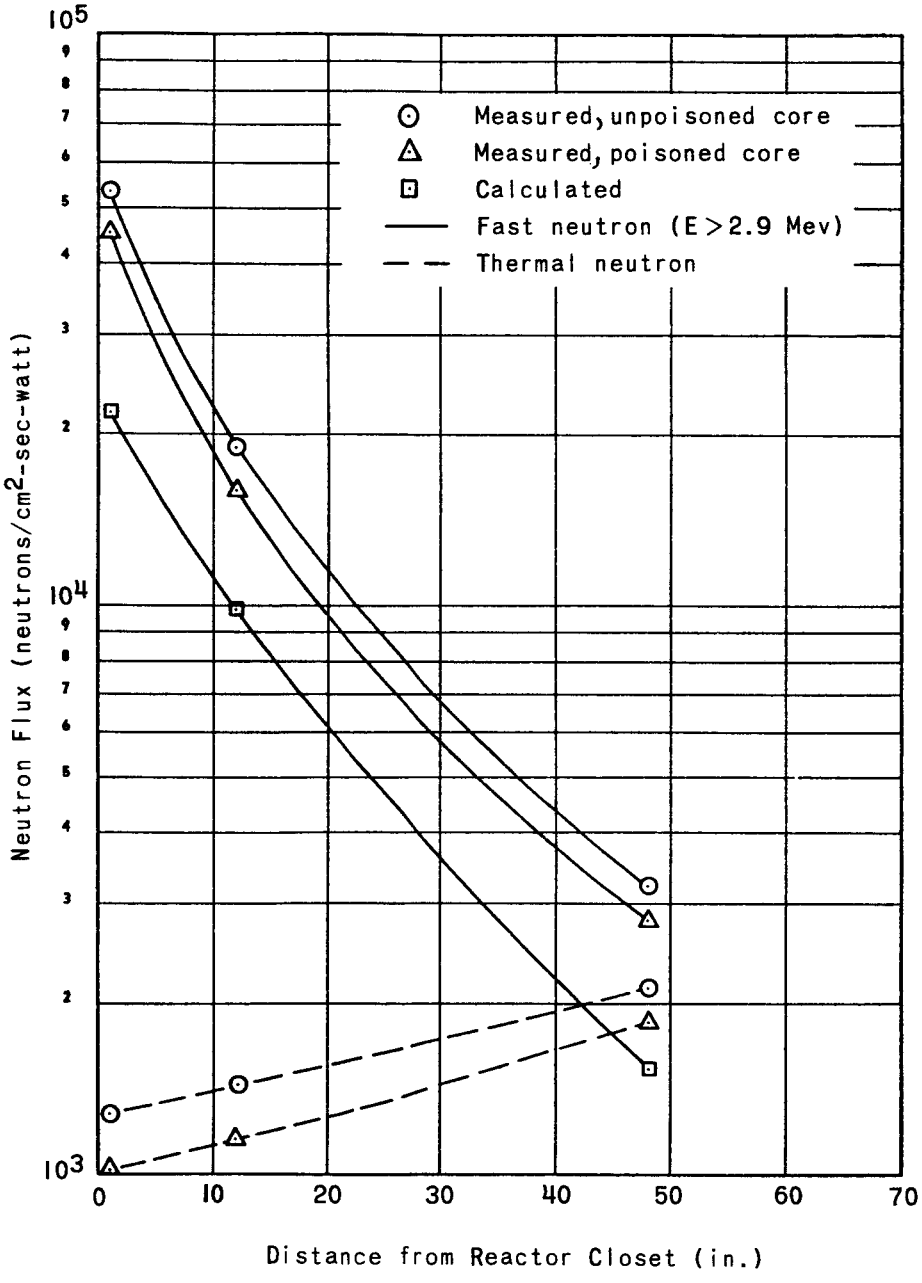

Figure 3.5 Average Neutron Flux on Rack Centerline: West Face

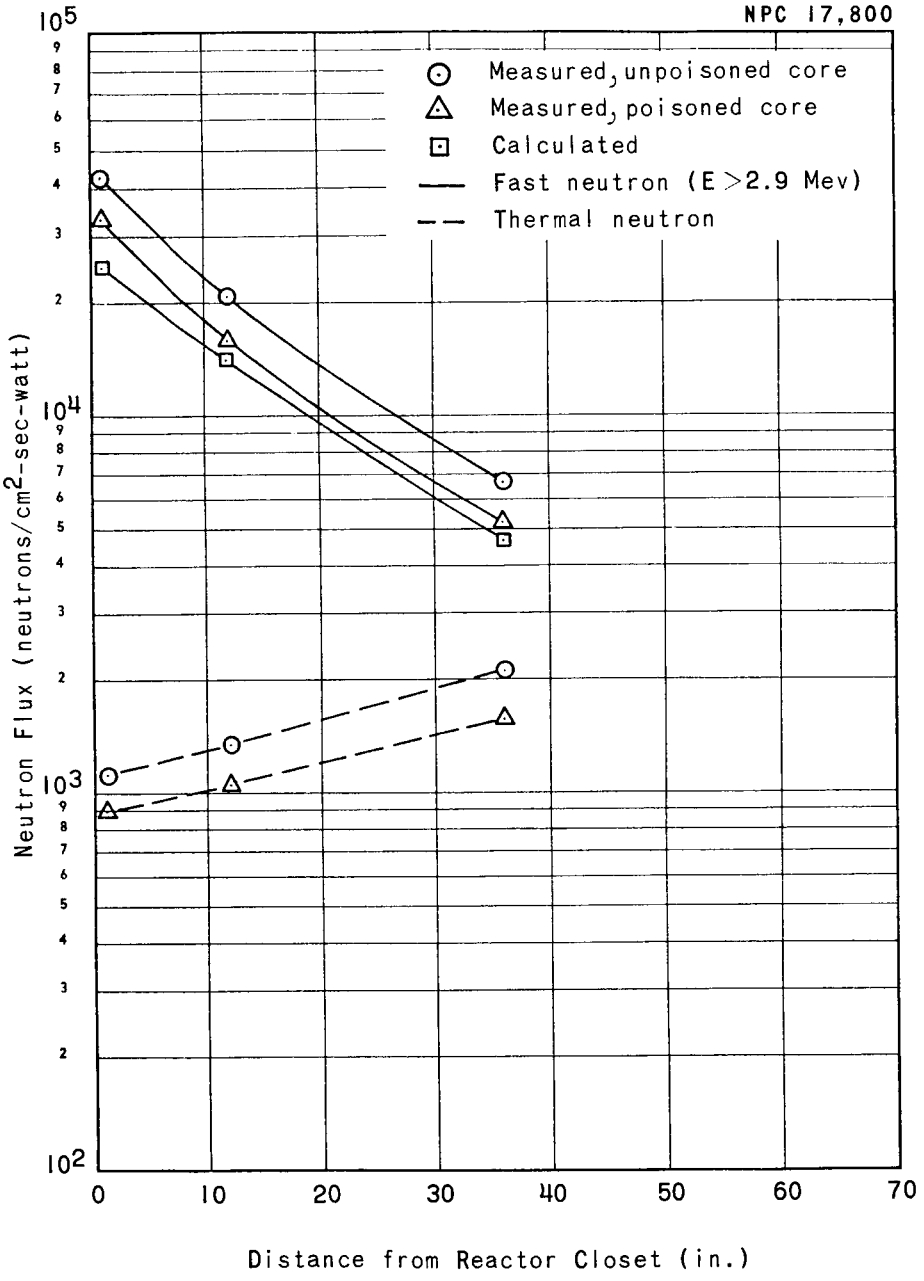

Figure 3.6 Average Neutron Flux 10 Inches Off Rack Centerline: North Face

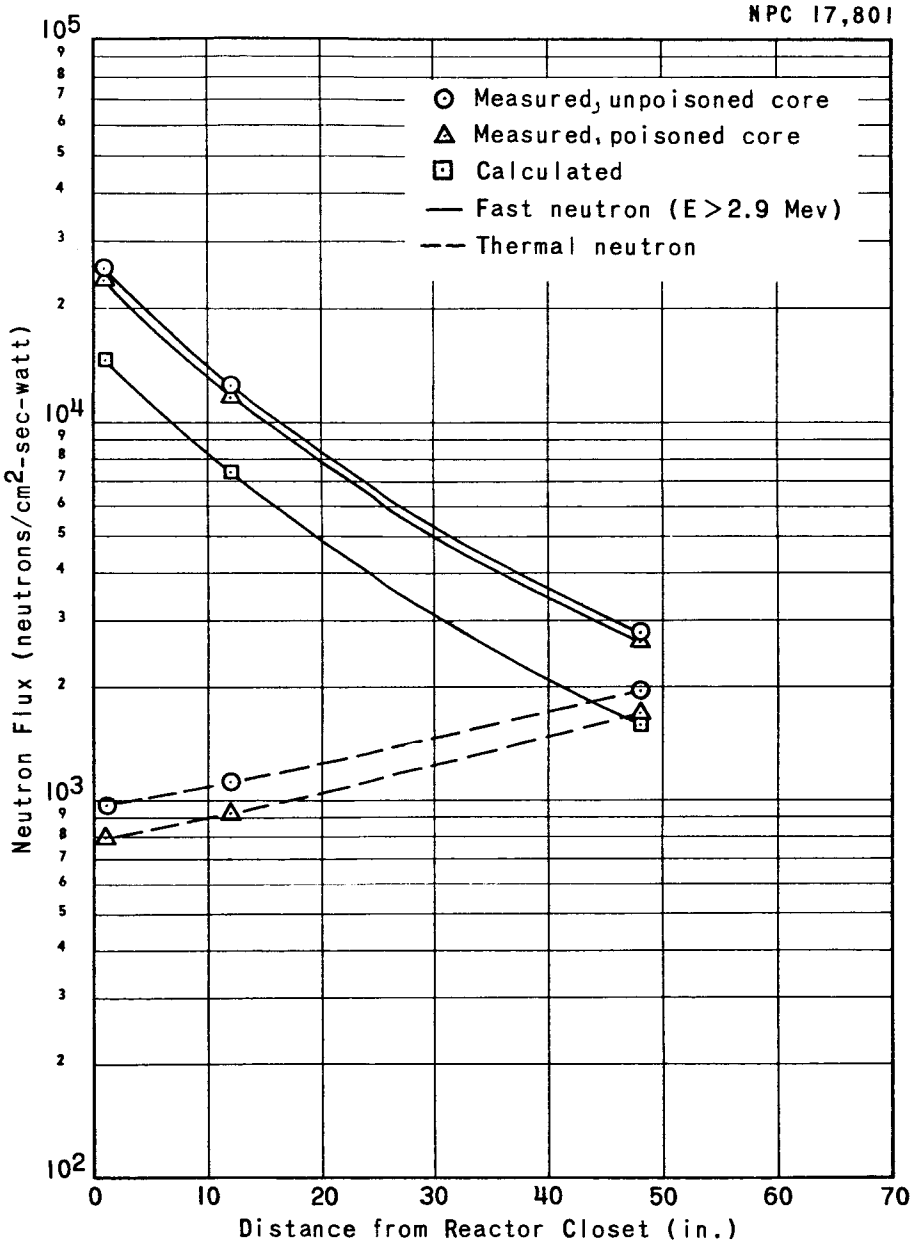

Figure 3.7 Average Neutron Flux 10 Inches Off Rack Centerline: East Face

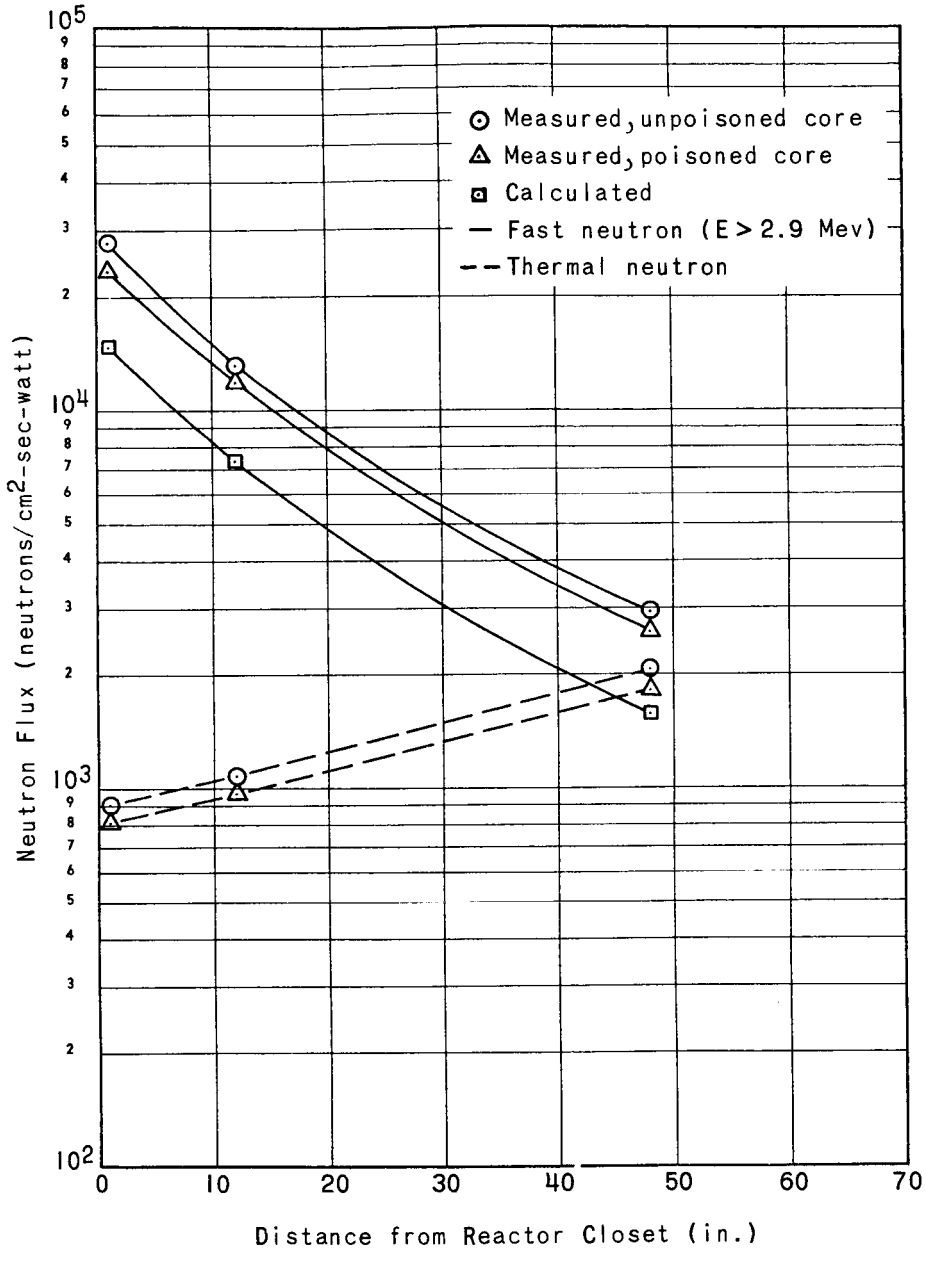

Figure 3.8 Average Neutron Flux 10 Inches Off Rack Centerline: West Face

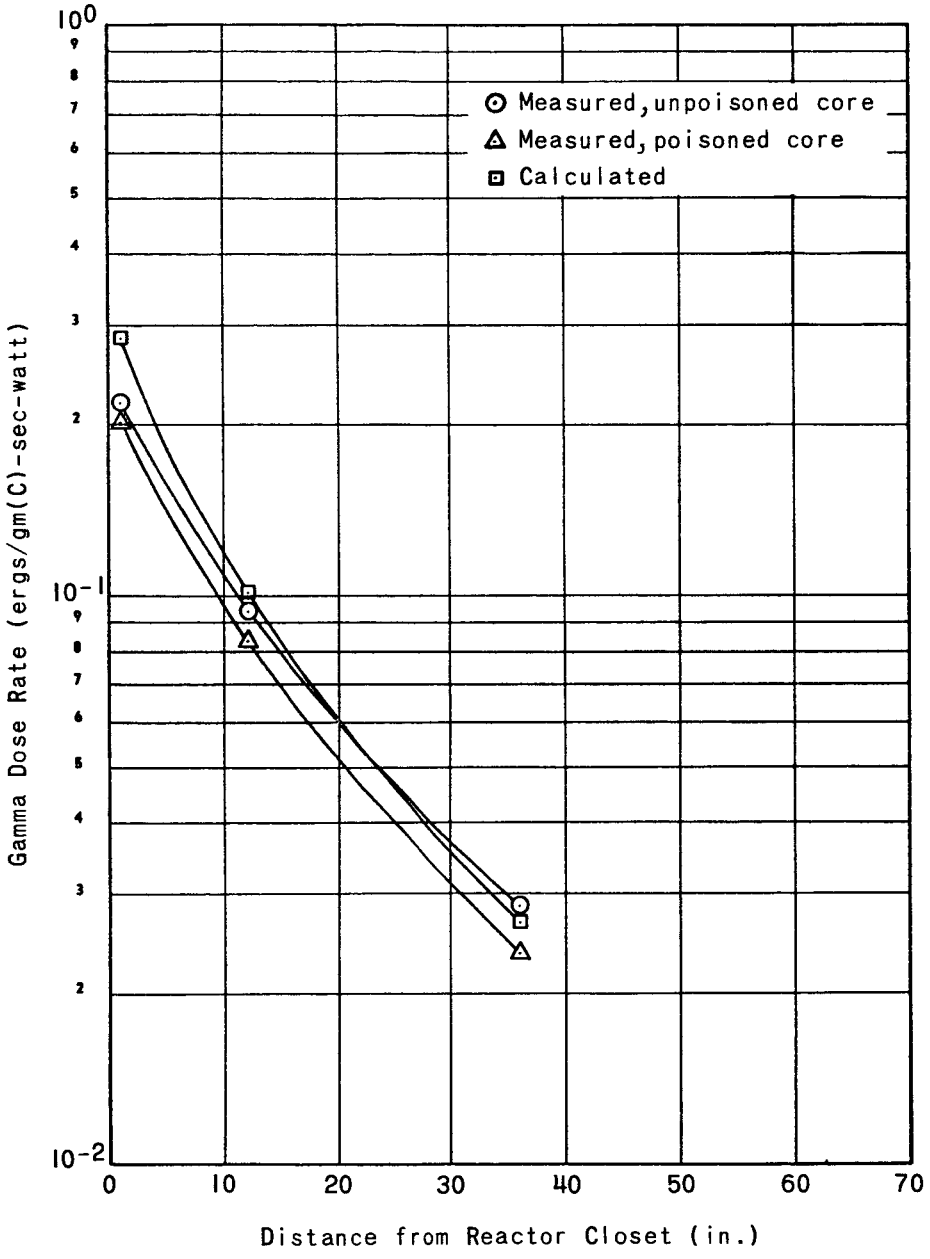

Figure 3.9 Average Gamma Dose Rate on Rack Centerline: North Face

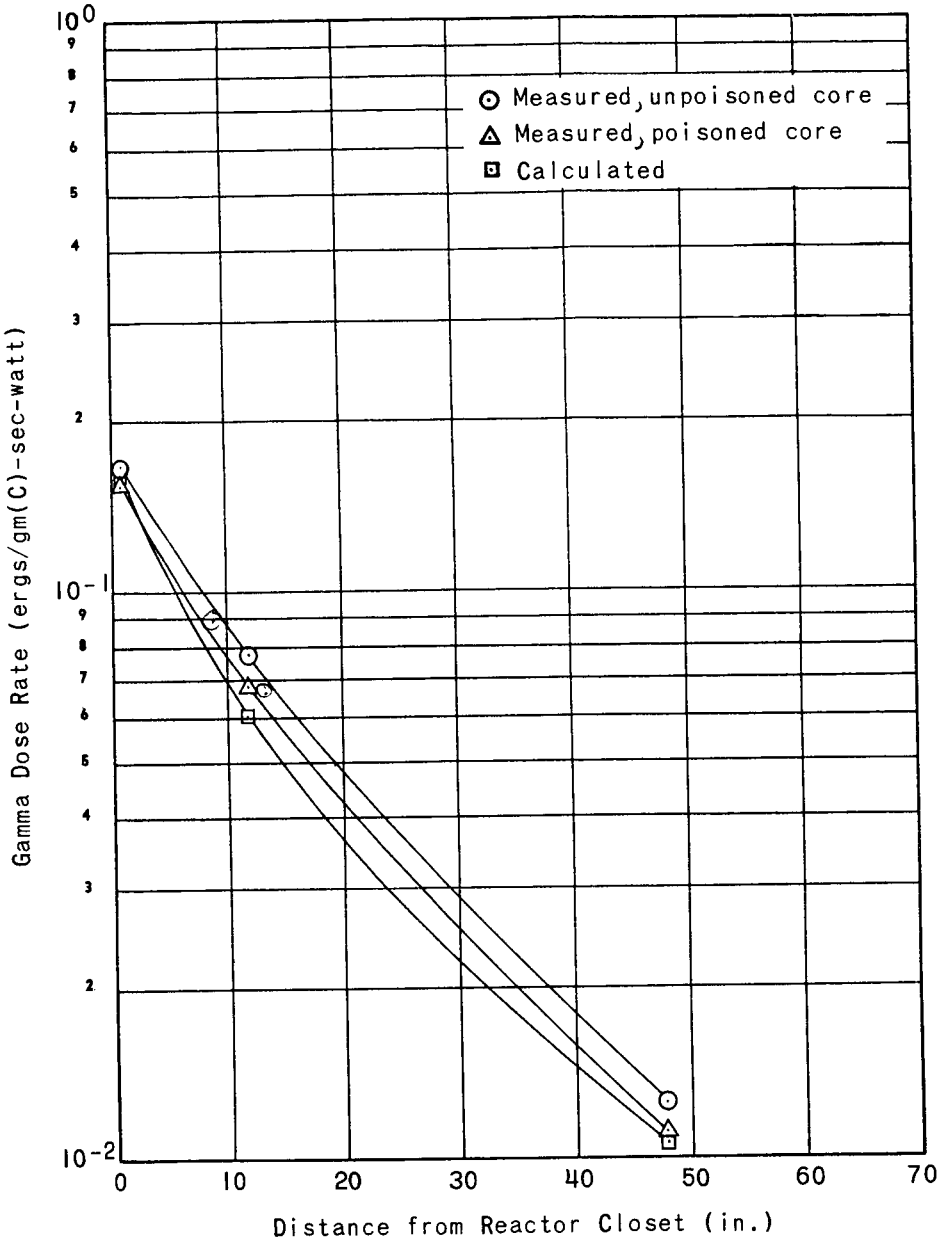

Figure 3.10 Average Gamma Dose Rate on Rack Centerline: East Face

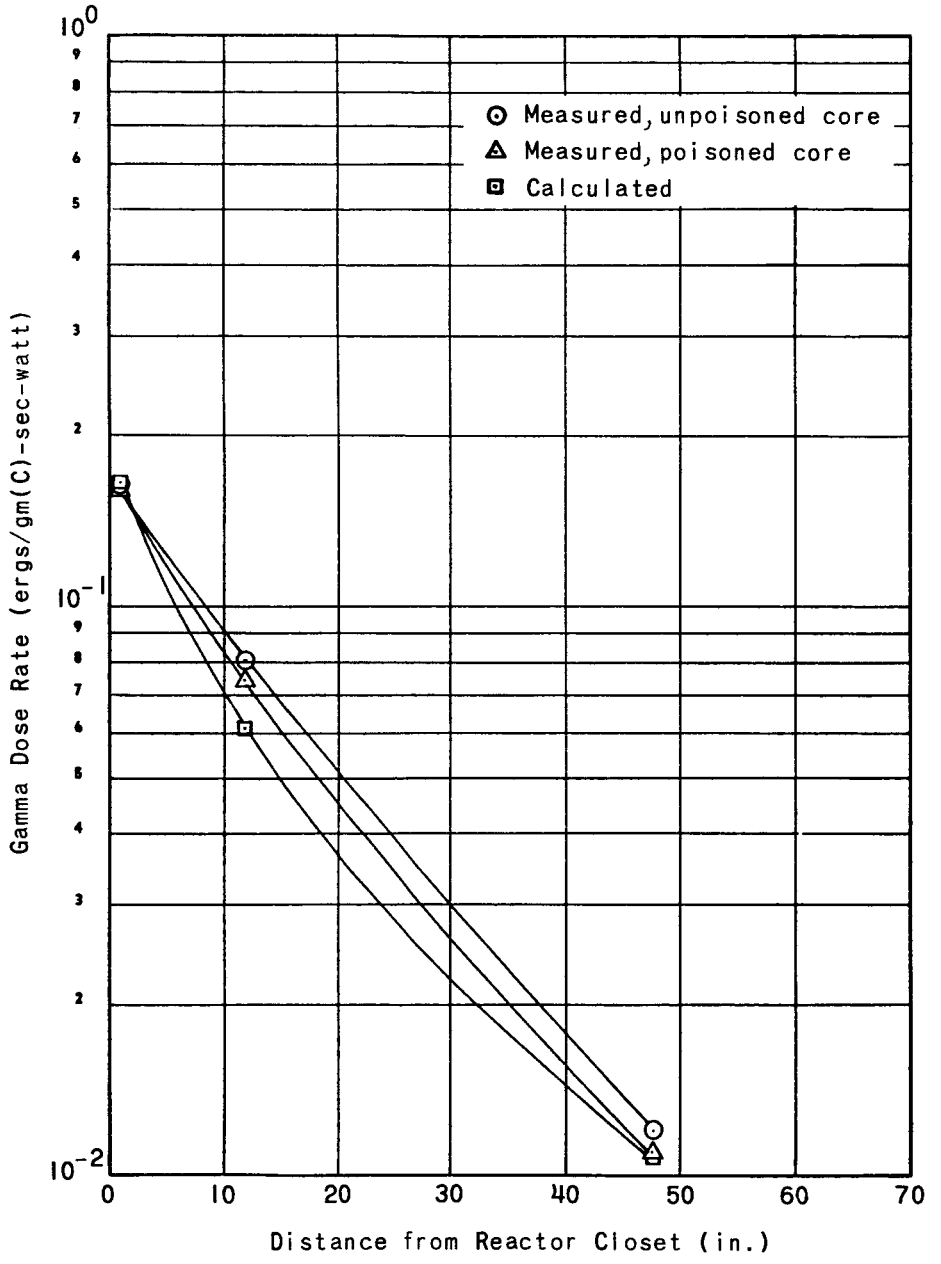

Figure 3.11 Average Gamma Dose Rate on Rack Centerline: West Face

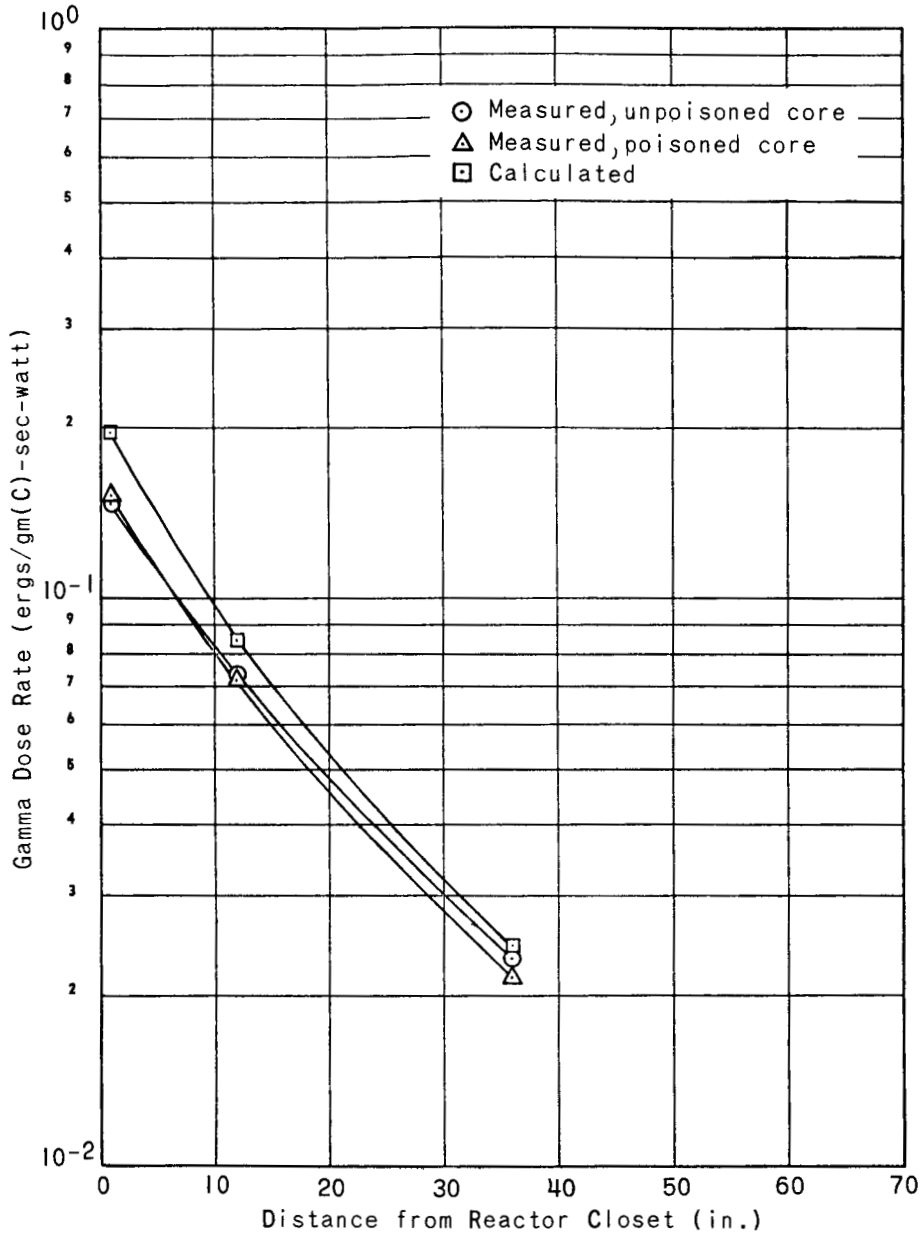

Figure 3.12 Average Gamma Dose Rate 10 Inches Off Rack Centerline: North Face

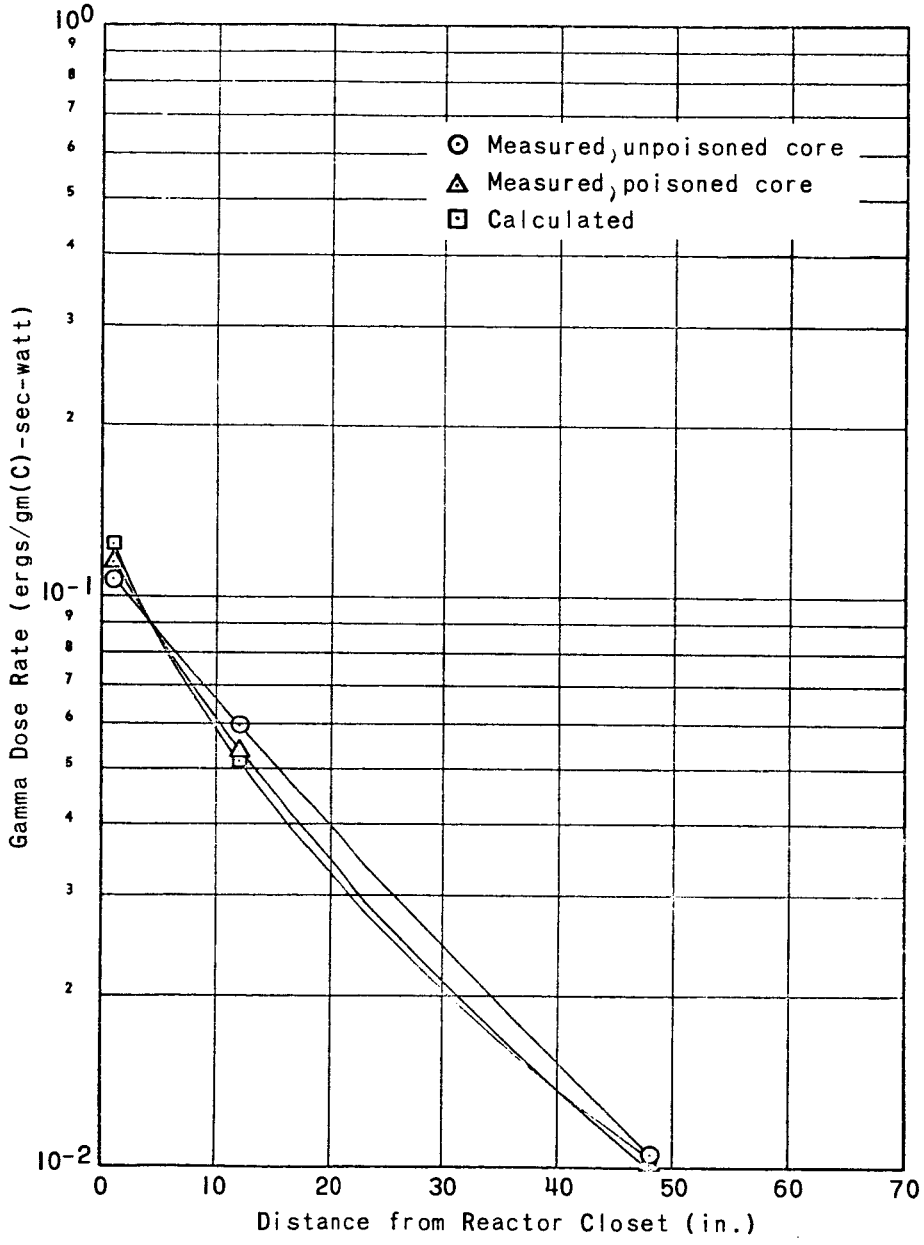

Figure 3.13 Average Gamma Dose Rate 10 Inches Off Rack Centerline: East Face

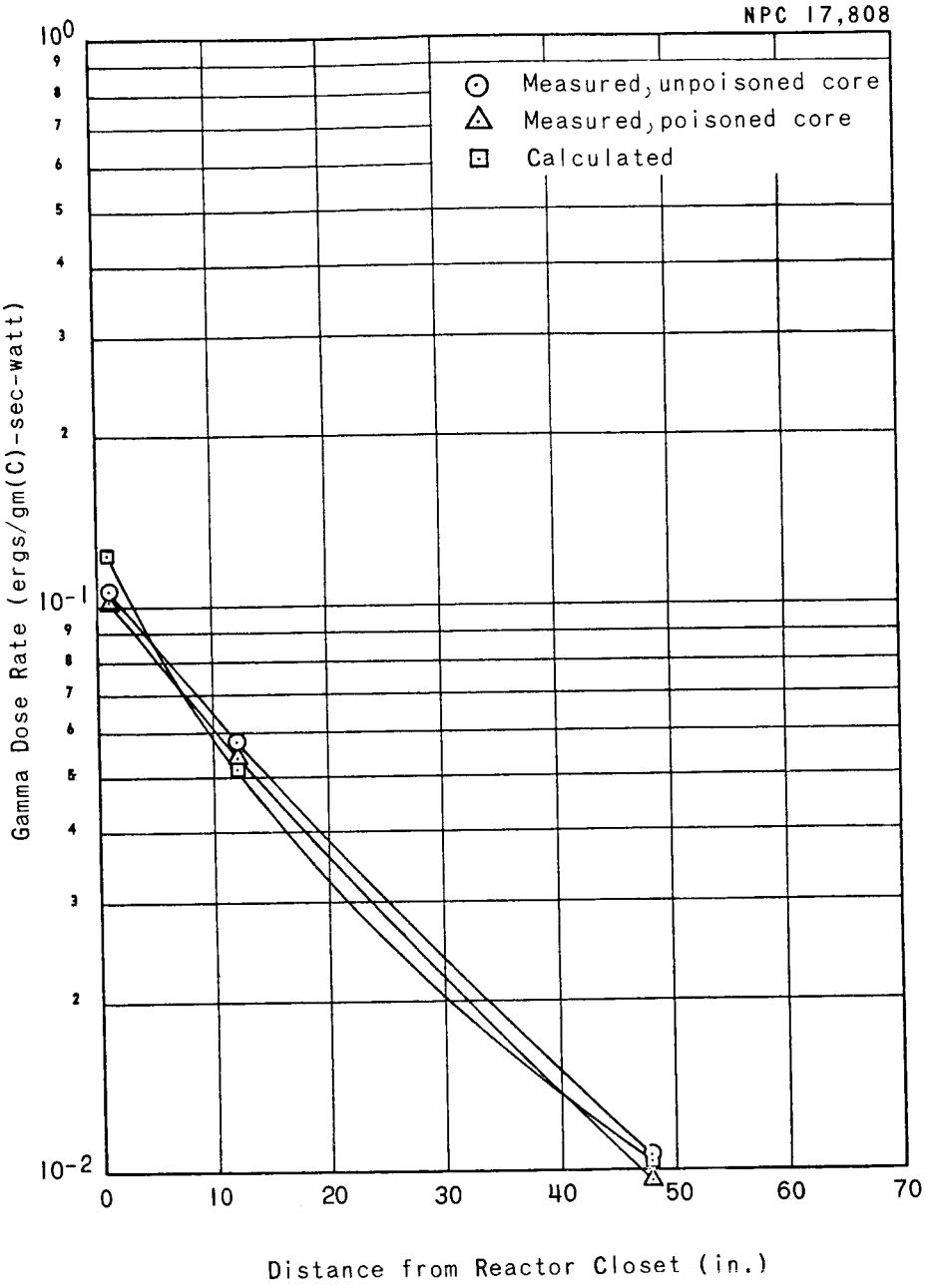

Figure 3.14 Average Gamma Dose Rate 10 Inches Off Rack Centerline: West Face

NPC 17,783
31-6919

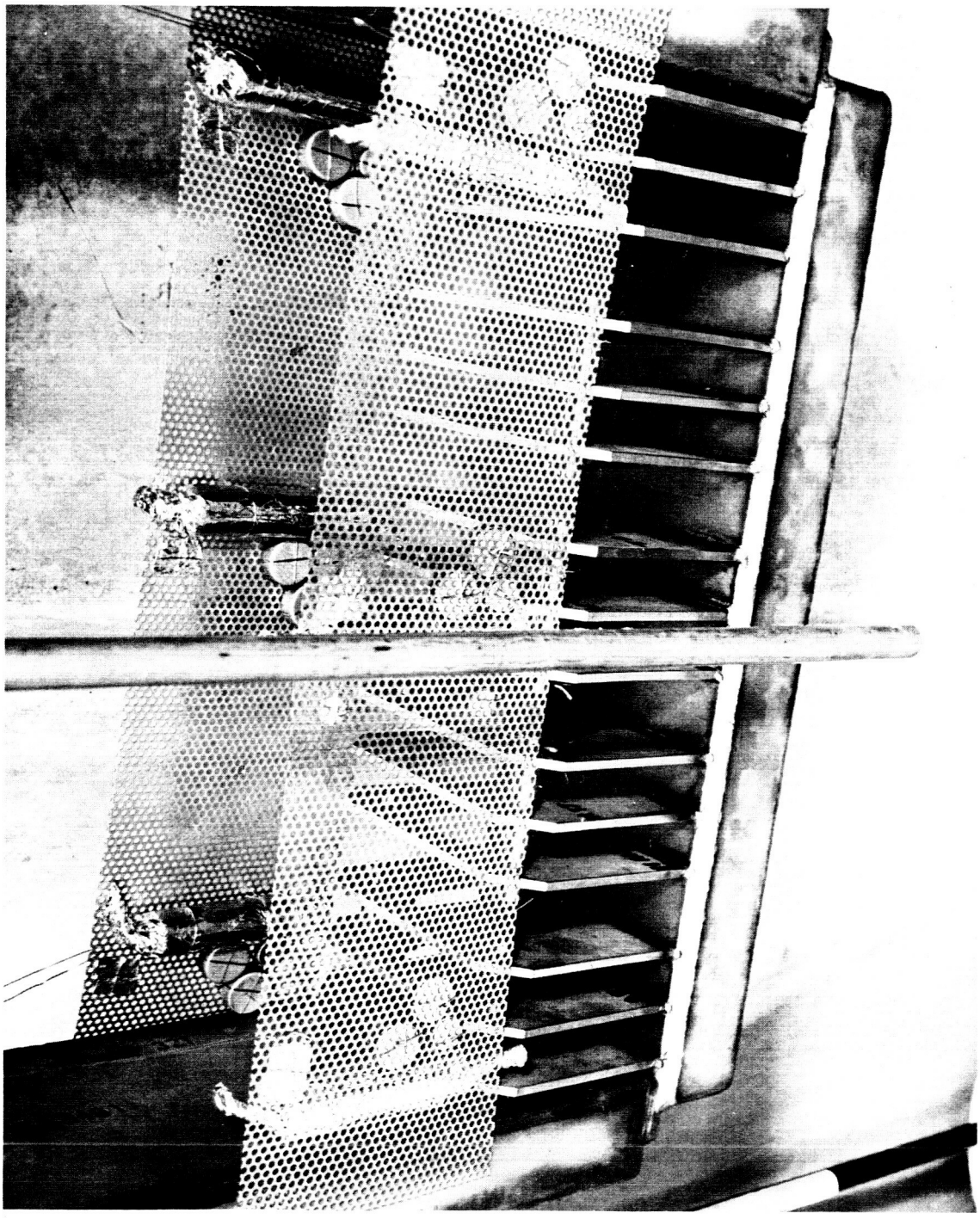

Figure 3.15 Mapping Dosimetry Mounted on Experimental Assembly

6, 8, and 10. Each packet contained one bare and one cadmium-covered silver-manganese foil to measure the thermal-neutron flux ($E < 0.48$ ev), one indium foil to measure the neutron flux for $E > 0.85$ Mev, one sulfur pellet to measure the neutron flux for $E > 2.9$ Mev, one aluminum foil to measure the neutron flux for $E > 8.1$ Mev, and a one nitrous-oxide dosimeter to measure the gamma dose. In addition to the above packets (which were inside the dewar during the run) packets consisting of one gamma dosimeter, one thermal detector, and one fast-neutron ($E > 2.9$ Mev) detector were mounted on the outside surfaces (front and back) of the dewars. These packets were positioned at the center of the dewar, just opposite a corresponding packet at rods 3 and 8 inside the dewar.

In the first run, the east dewar was filled with water and the north dewar contained static air at atmospheric pressure and ambient temperature. In the second run (which used the same dosimetry layout as described above), only the north assembly, with LN_2-filled dewar, was irradiated.

Past experience with dosimetry measurements on the GTR has established the reliability of using a definite ratio of east-to-west and east- or west-to-north dose rates in air at given distances from the reactor face on the core centerline. For fast neutrons ($E > 2.9$ Mev), the east-to-west ratio is 1:1 and the east- or west-to-north ratio is 1:1.7. For gamma radiation, the east-to-west ratio is 1:1 and the east- or west-to-north ratio is 1:1.2. Reiliability of these values is considered to be well within the limits of reproducibility of successive measurements for both neutrons and gamma rays. The north-to-east-

or-west ratio (1.7:1) is based on a 4-in. thickness of water between the core and the inside face of the closet. This ratio can be increased by moving the reactor north, into the closet, thus reducing this water thickness to 2 inches.

With these ratios and with the data taken on the above-described mapping run, it is possible to determine both the neutron and gamma dose rates in the experimental assemblies at all the irradiation positions for all three dewar environments: water, air, and liquid nitrogen. Water was used in the east dewar to simulate the neutron attenuation that would take place in liquid hydrogen, and data from this dosimetry are considered suitable for predicting dose rates in an LH_2-filled dewar. The usual environment in the dewars for irradiations at NARF is either air, LN_2, or LH_2.

Data from the mapping runs are shown in Tables 3.1 through 3.3 and are plotted in Figures 3.16 through 3.21.

Figures 3.16 through 3.18 are plots of the neutron fluxes under the three environments. Fast fluxes in the east, west, or north dewar under any of the three environments can thus be determined either by referring to the appropriate curves or by multiplying or dividing a particular data point on a curve by the factor 1.7.

Figures 3.19 through 3.21 are plots of gamma dose rates under the three environments. Like the above-described approach for neutron fluxes, the gamma dose rates in the east, west, or north dewar under any of the three environments can be determined either by reference to the appropriate curve or by calculation. Gamma dose rates for a particular environment and irradiation

Table 3.1

Experimental-Assembly Mapping Run: East Dewar, H_2O-Filled

Dosimeter Location		Neutron Flux (n/cm^2-sec-watt)				Gamma Dose Rate (ergs/gm(C) -hr-watt)
		E > 0.48 ev	E > 0.85 Mev	E > 2.9 Mev	E > 8.1 Mev	
Outside front face of dewar	Front of Rod 1	-	-	-	-	-
	Front of Rod 3	1.10(4)	-	4.09(4)	-	9.5(2)
	Front of Rod 5	-	-	-	-	-
Inside of dewar	At Rod 1	6.89(4)	2.22(4)	1.06(4)	4.22(2)	2.8(2)
	At Rod 3	1.17(5)	3.86(4)	1.51(4)	5.85(2)	3.9(2)
	At Rod 5	6.98(4)	2.84(4)	1.18(4)	4.73(2)	4.0(2)
Inside of dewar	At Rod 6	1.65(4)	2.86(3)	1.19(3)	1.29(2)	1.3(2)
	At Rod 8	2.19(4)	3.19(3)	1.74(3)	1.13(2)	1.8(2)
	At Rod 10	1.40(4)	3.42(3)	1.42(3)	9.57(1)	1.3(2)
Outside back face of dewar	Back of Rod 6	-	-	-	-	-
	Back of Rod 8	1.13(3)	-	3.19(2)	-	9.0(1)
	Back of Rod 10	-	-	-	-	-

Table 3.2

Experimental-Assembly Mapping Run: North Dewar, Air-Filled

Dosimeter Location		Neutron Flux (n/cm^2-sec-watt)				Gamma Dose Rate (ergs/gm(C) -hr-watt)
		E > 0.48 ev	E > 0.85 Mev	E > 2.9 Mev	E > 9.1 Mev	
Outside Front Face of Dewar	Front of Rod 1	-	-	-	-	-
	Front of Rod 3	1.83(3)	-	6.26(4)	-	1.2(3)
	Front of Rod 5	-	-	-	-	-
Inside of Dewar	At Rod 1	-	5.99(4)	2.52(4)	9.16(2)	4.7(2)
	At Rod 3	1.65(3)	6.71(4)	2.79(4)	1.03(3)	5.6(2)
	At Rod 5	2.28(3)	5.49(4)	2.30(4)	8.19(2)	4.9(2)
Inside of Dewar	At Rod 6	2.31(3)	1.22(5)	1.55(4)	6.30(2)	3.2(2)
	At Rod 8	2.19(3)	4.87(4)	1.83(4)	7.29(2)	3.4(2)
	At Rod 10	1.86(3)	4.01(4)	1.58(4)	6.08(2)	3.3(2)
Outside Back Face of Dewar	Back of Rod 6	-	-	-	-	-
	Back of Rod 8	2.04(3)	-	8.76(3)	-	1.4(2)
	Back of Rod 10	-	-	-	-	-

Table 3.3

Experimental-Assembly Mapping Run: North Dewar, LN_2-Filled

Dosimeter Location		Neutron Flux (n/cm²-sec-watt)				Gamma Dose Rate (ergs/gm(C) -hr-watt)
		E > 0.48 ev	E > 0.85 Mev	E > 2.9 Mev	E > 8.1 Mev	
Outside Front Face of Dewar	Front of Rod 1	-	-	-	-	-
	Front of Rod 3	4.90(3)	-	6.59(4)	-	1.2(3)
	Front of Rod 5	-	-	-	-	-
Inside of Dewar	At Rod 1	2.46(3)	-	2.60(4)	8.90(2)	1.0(3)
	At Rod 3	3.79(3)	8.10(4)	2.88(4)	9.75(2)	1.6(3)
	At Rod 5	2.59(3)	7.03(4)	2.45(4)	8.90(2)	7.2(2)
Inside of Dewar	At Rod 6	-	3.07(4)	1.03(4)	4.00(2)	6.8(2)
	At Rod 8	1.70(3)	3.76(4)	1.31(4)	5.08(2)	3.9(2)
	At Rod 10	1.07(3)	-	1.03(4)	4.01(2)	2.4(2)
Outside Back Face of Dewar	Back of Rod 6	-	-	-	-	-
	Back of Rod 8	1.22(3)	-	3.69(3)	-	8.6(1)
	Back of Rod 10	-	-	-	-	-

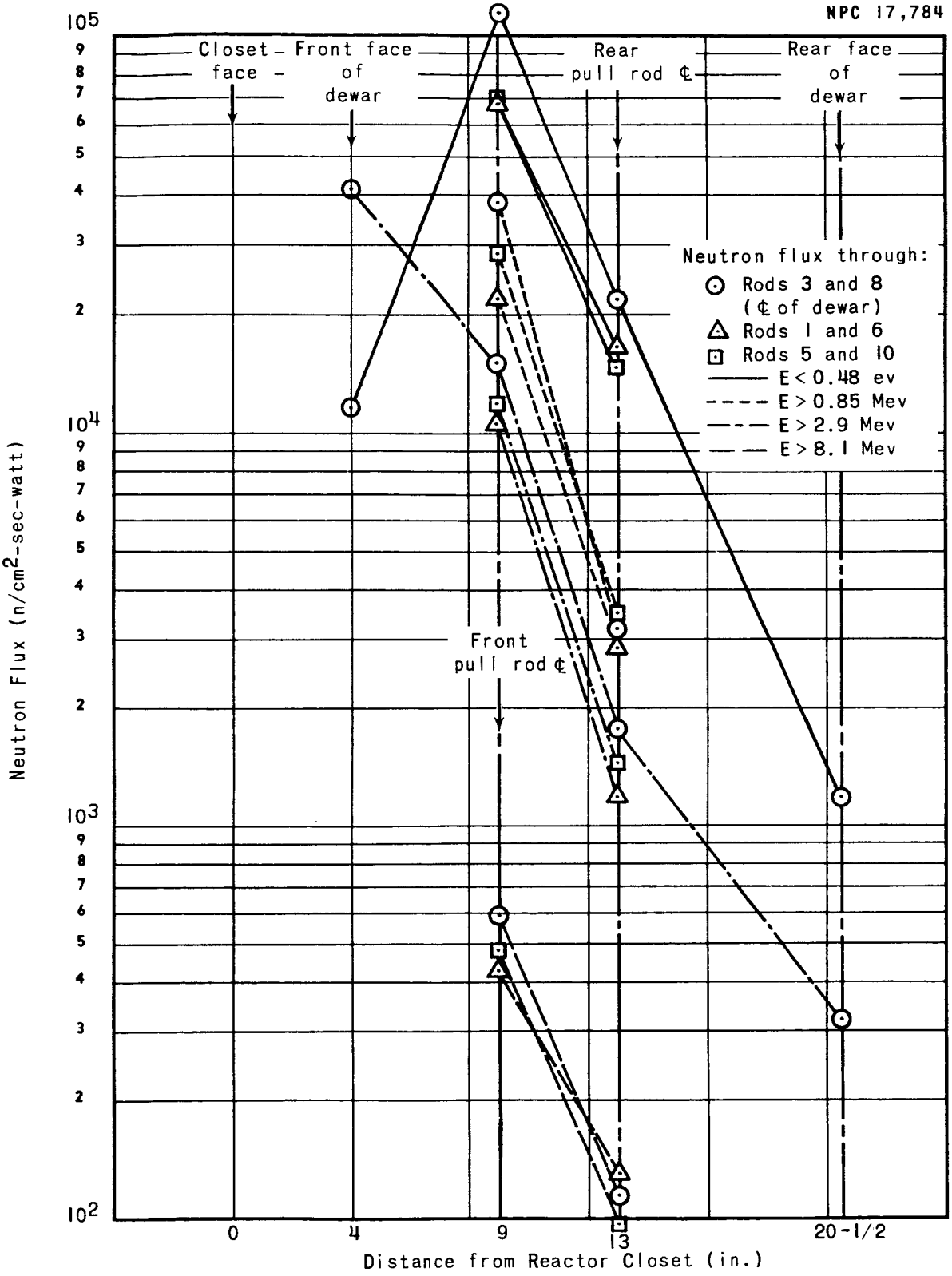

Figure 3.16 Neutron Flux vs Distance from Reactor: East Dewar, H_2O-Filled

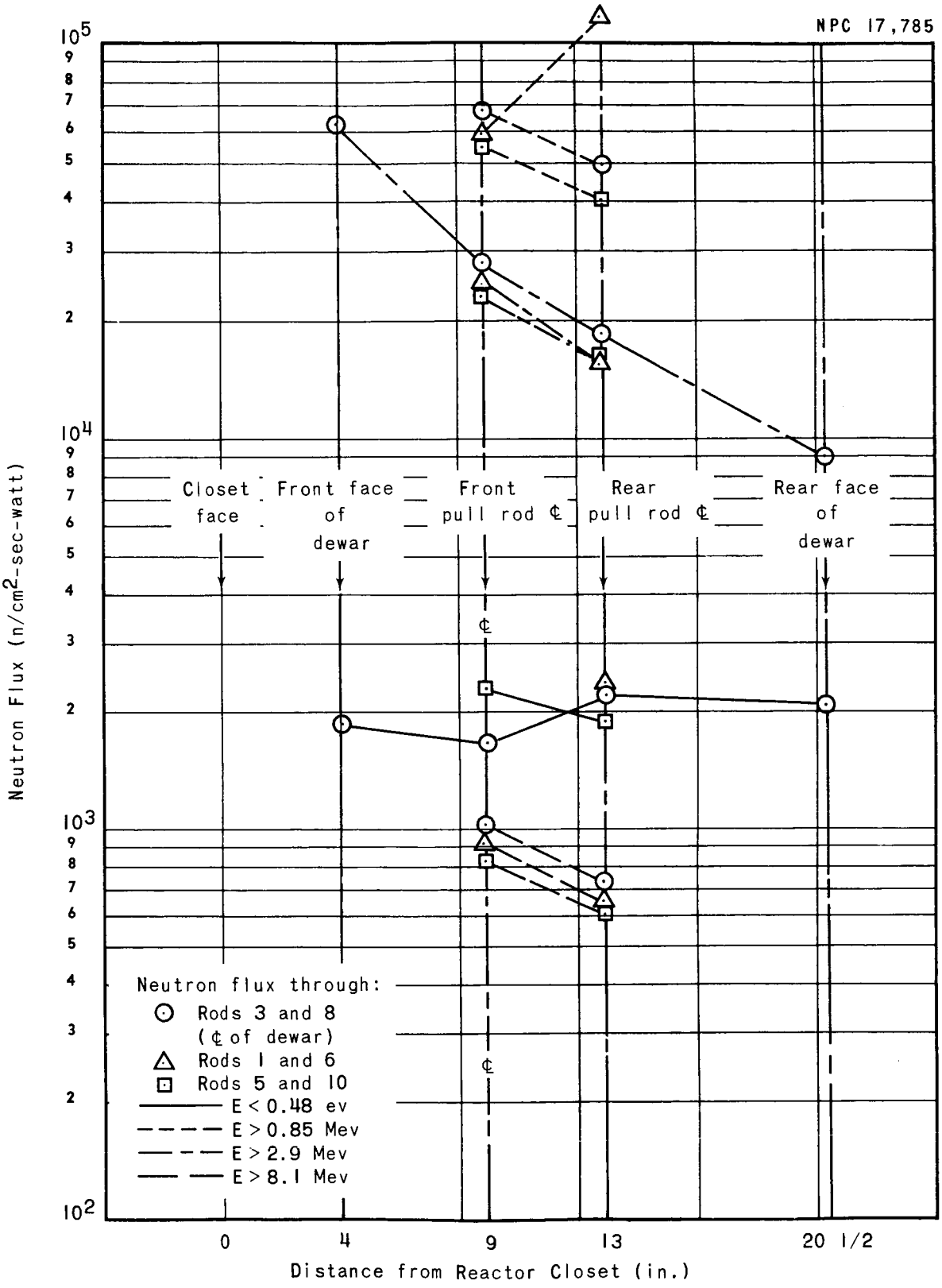

Figure 3.17 Neutron Flux vs Distance from Reactor: North Dewar, Air-Filled

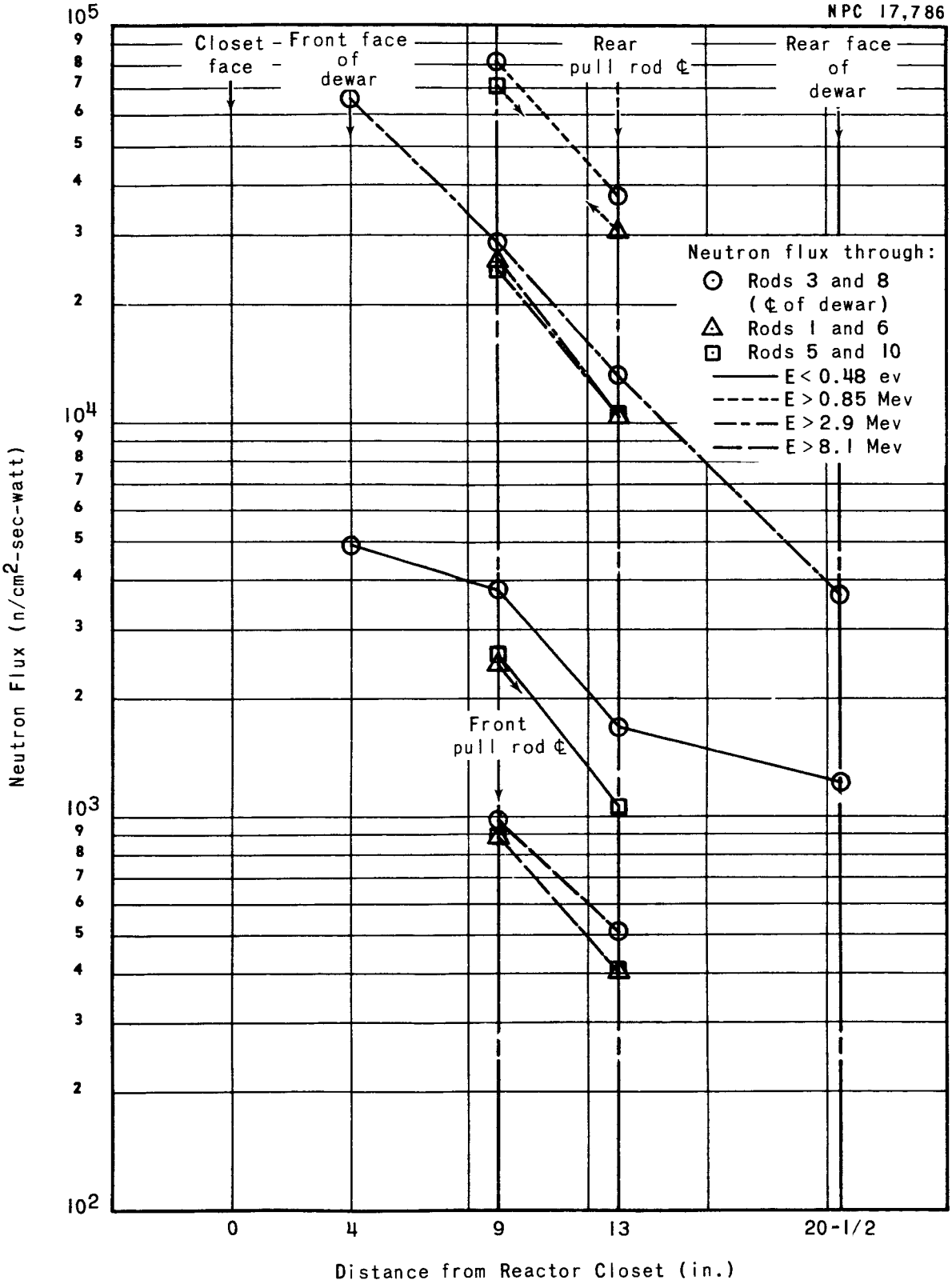

Figure 3.18 Neutron Flux vs Distance from Reactor: North Dewar, LN_2-Filled

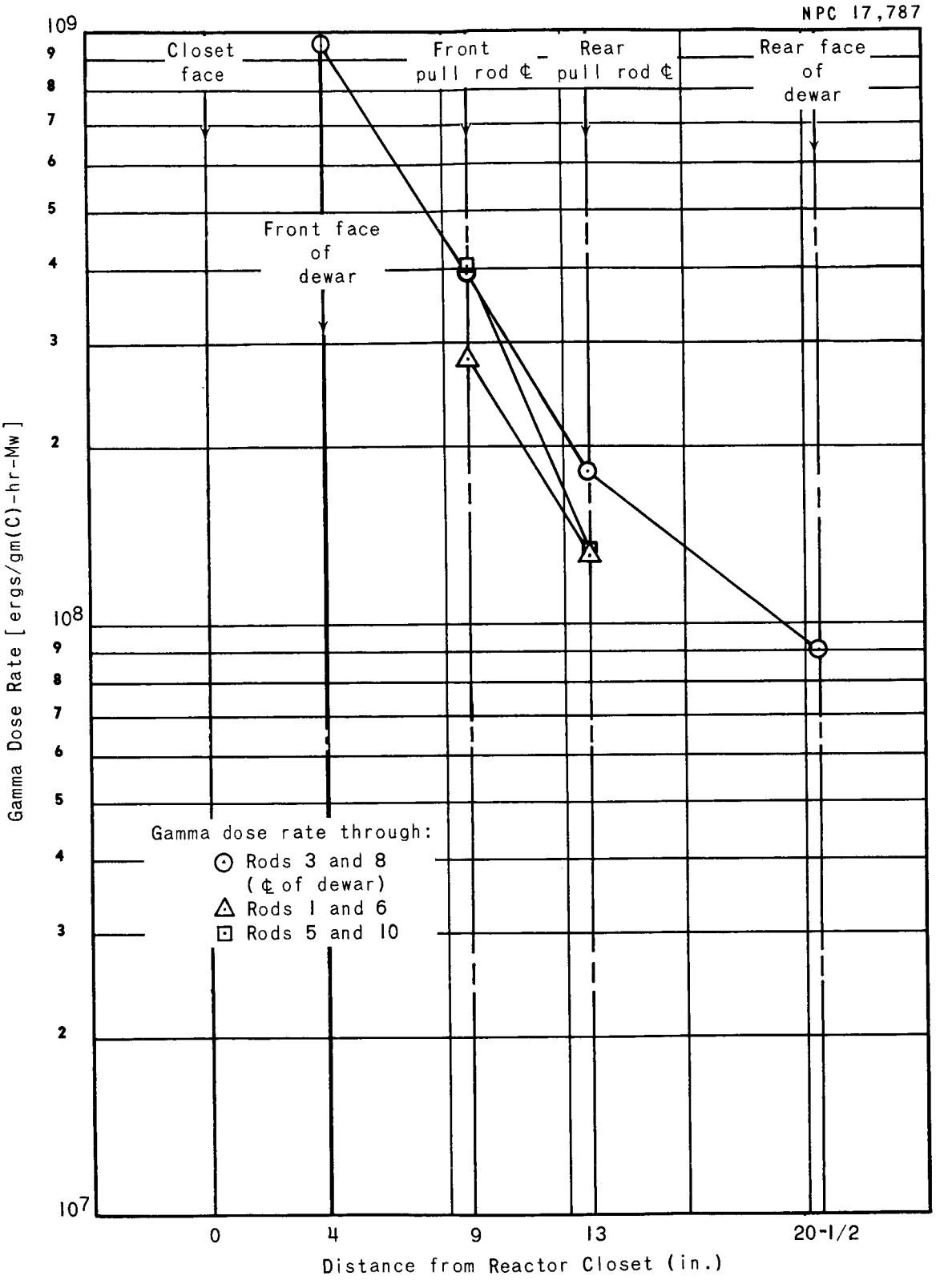

Figure 3.19 Gamma Dose Rate vs Distance from Reactor: East Dewar, H_2O-Filled

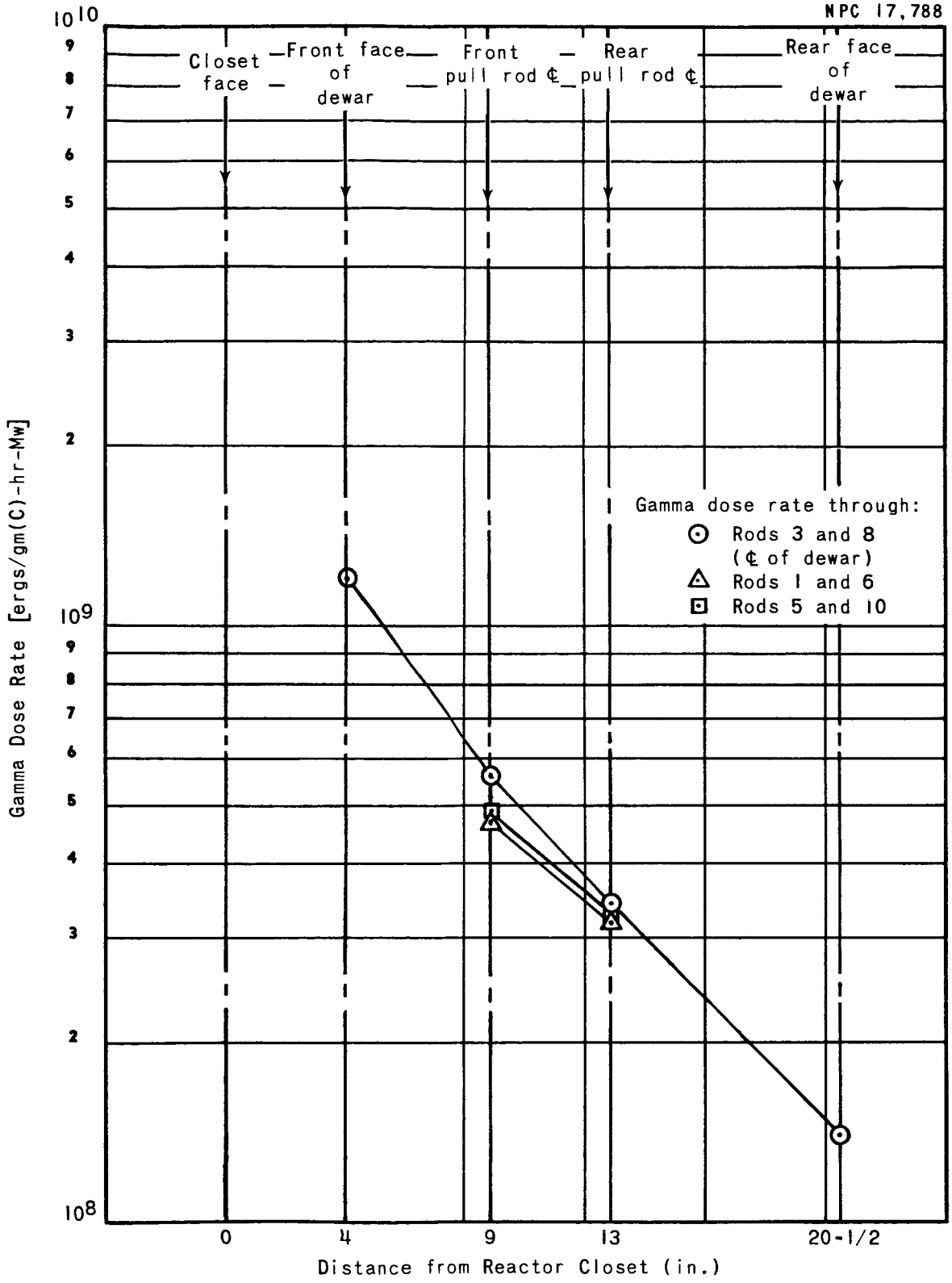

Figure 3.20 Gamma Dose Rate vs Distance from Reactor: North Dewar, Air-Filled

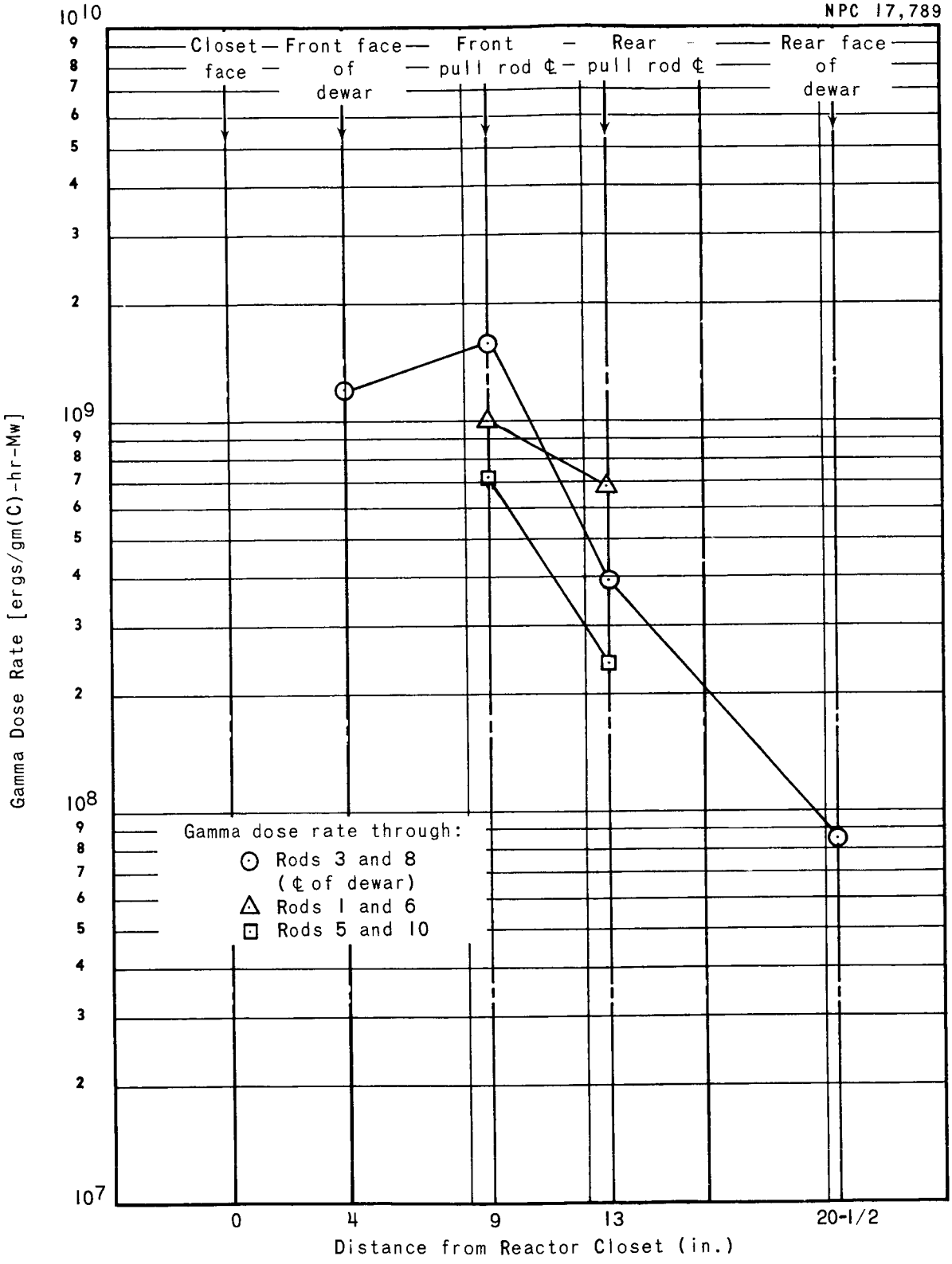

Figure 3.21 Gamma Dose Rate vs Distance from Reactor: North Dewar, LN_2-Filled

position not used in the mapping runs can be determined by multiplying or dividing a particular recorded data point by the factor 1.2.

No radical departures from anticipated neutron-flux values are indicated in Figures 3.16 through 3.18. The high thermalizing effect of water can be noted in data taken from the water-filled dewar. Reference to Figures 3.17 and 3.18 indicate nothing more than normally expected mass and distance attenuation of neutron fluxes, thus inferring little or no low-temperature effects on neutron dosimetery in the LN_2-filled dewar.

Gamma dose-rate data recorded in the mapping runs were reasonable and generally according to expectations. As anticipated, reaction of N_2O gamma dosimeters irradiated while submerged in LN_2 was erratic. This is indicated in Figure 3.21. Based on the gamma dose rates recorded for the front and rear outside faces of the dewar and the dose-rate curve for the air-filled north dewar, curves for the dose rates through the LN_2-filled dewar which were considered to be correct were drawn into Figure 3.21 as dashed lines. These values will be used in determining specimen locations for future LN_2 irradiations until such time when gamma dosimetry suitable for use at cryotemperatures has been developed.

3.5 Preirradiation Materials Tests

Preirradiation tests at ambient-air, LN_2, and LH_2 temperatures were scheduled for each material in the program. To date, tests on most of the materials at ambient-air and LN_2 temperatures have been completed. A general discussion of the results of the completed tests for each material is given below.

Adhesives

Material A: AF-40. The ambient-air, preirradiation (or control) specimens for this material were tested for lap-shear strength. Data were consistent, with lap-shear-strength values running around 3000 psi. At LN_2 temperature, the lap-shear data were not quite as consistent, and forces-to-break were much lower, averaging about 2000 psi.

Material B: 422J. At ambient-air temperature, the lap-shear control specimens broke at about 1250 psi. At the LN_2 temperature, the lap-shear strength went up to about 1500 psi.

Seals

Material C: Viton B. This material was to be tested in O-ring form for sealing characteristics. The O-rings were only recently received at GD/FW, however; so tests have been postponed until later in the year.

Material D: Polymer SP. This material was formed into dumbbell-type specimens (see Fig. 3.7, Ref. 3). During tests under all conditions, every specimen broke in the vicinity of the doublers; so no data were recorded. The specimens are being redesigned for possible subsequent tests.

Thermal Insulations

Material E: Stafoam AA-402. The thermal conductivity testers for this material have not been completed and tests have been delayed to a later date.

Material F: CPR-20. The thermal conductivity testers for this material have not been completed and tests have been delayed to a later date.

Material G: CPR-1021. The thermal conductivity testers for this material have not been completed and tests have been delayed to a later date.

Electrical Insulations

Material H: Geon 8800. This material tested quite satisfactorily at ambient-air temperature. Stress-strain, ultimate elongation, and ultimate tensile strength (approximately 2720 psi) measurements were obtained. At LN_2 temperatures, however, all the dumbbell-type specimens shattered between the aluminum doublers during testing and no data were obtained. The specimens are being redesigned for possible rerun in future tests.

Material I: Duroid 5600. These dumbbell-type specimens tested satisfactorily. At ambient-air temperature, the ultimate tensile strength averaged 2800 psi. At LN_2 temperature, this strength was increased to about 4300 psi.

Material J: Milimene-Glass 6038. Specimens of this material, in dumbbell-type form, tested quite satisfactorily. The ultimate tensile strength at ambient-air temperature averaged 58,000 psi. At LN_2 temperature the ultimate strength jumped to 115,000 psi.

Structural Laminate

Material K: CTL-91-LD. This material tested satisfactorily at both temperatures. The ultimate tensile strength was about 29,500 psi at ambient-air temperature and about 44,700 psi at LN_2 temperature.

Material L: DC-2104. This laminate also tested satisfactorily at ambient-air temperature, but the doublers failed to stay on the specimens during LN_2 tests. The ultimate tensile strength at ambient-air temperature was 22,400 psi and, at LN_2 temperature, about 60,000 psi before the doublers slipped off.

Potting Compounds

Material M: Epon 828/Z. Tests for both potting compounds consisted of potting standard 22-gage bookup wire in the material to a depth of 1/2 in. and, after the system hardened, pulling the wires out of the compound and measuring the maximum break-out load. Good data resulted from tests run on the ambient-air specimens, maximum break-out load averaging about 37 lb. These loads dropped somewhat for test specimens submerged in LN_2.

Material N: EC-2273 B/A. Data for specimens of this material were similar to those taken for Material M, except that the LN_2-specimen break-out load was higher than that for the ambient-air specimens.

Sealants

Material O: EC-1949. This material was tested for T-peel strength. Specimen shape and size are shown in Reference 3. The maximum load required to pull the upper and lower alumium adherents apart was recorded. This amounted to about 60 lb for the unirradiated ambient-air specimens. No data were obtained from the specimens submerged in LN_2, because the material failed to adhere to the aluminum at this temperature.

Material P: EC-1663. Specimens and tests for this material were identical to those for Material O. The ambient-air loads were down to about 35 lb, but some adherence to the aluminum was maintained at LN_2 temperature, with loads of about 32 lb being recorded.

The ambient-air tests were conducted in the IML, with the specimens mounted directly in the Instron machine. The LN_2 tests were conducted with the west experimental assembly, the Instron machine, and the interconnecting hydraulic servosystem. The cryogen chamber of the assembly was kept full of boiling LN_2 during the tests. The specimen arrangement in the assembly prior to start of the tests is shown in Figures 3.22 and 3.23. These photographs are views of pull rods 1 through 5 and 6 through 10, respectively.

3.6 Irradiation Tests

The irradiation tests were conducted in the Radiation Effects Testing System at NARF (see Figures 3.24 and 3.25), with the GTR as the radiation source. For the ambient-air temperature tests, the expanded-metal tray rack was used and specimens were mounted as shown in Figures 3.26, 3.27, and 3.28. The required gamma doses in ergs/gm(C) (as shown in the upper right hand corner of the photographs) were obtained by judicious placement of the expanded metal trays in the rack and by removing the different trays from the radiation field at specified times. The high-dose tray, for instance, required an irradiation time of 33 hr, with the reactor operated at a power level of 3 Mw. Table 3.4 gives the specimen location and irradiation times during the ambient-air run. Thermocouples were mounted on specimens in the different trays to measure the range of temperatures of specimens during the irradiation.

NPC 17,790
31-6980

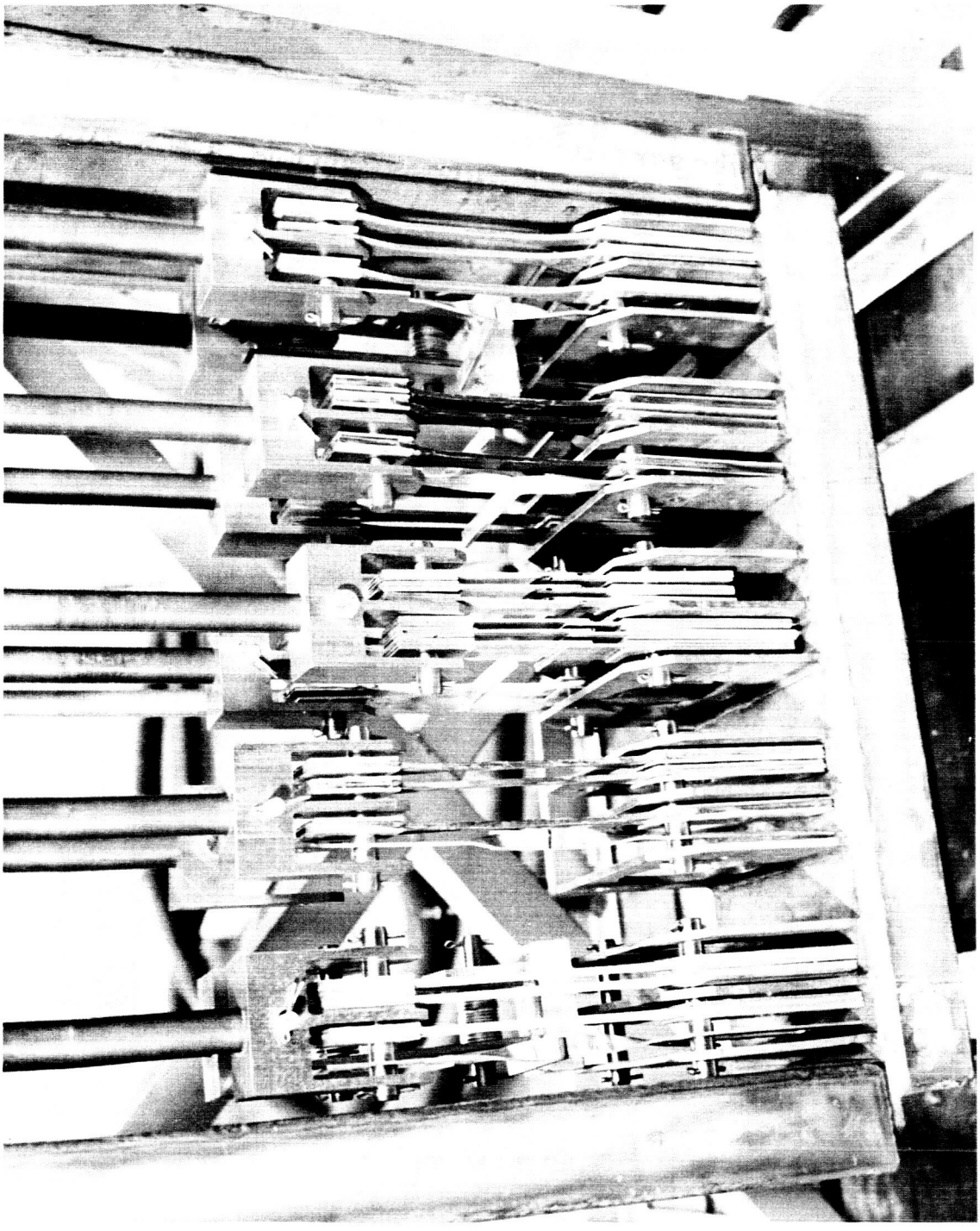

Figure 3.22 Specimen Mounting Arrangement for LN_2 Irradiation: Low Dose, Reactor Side

NPC 17,791
31-6981

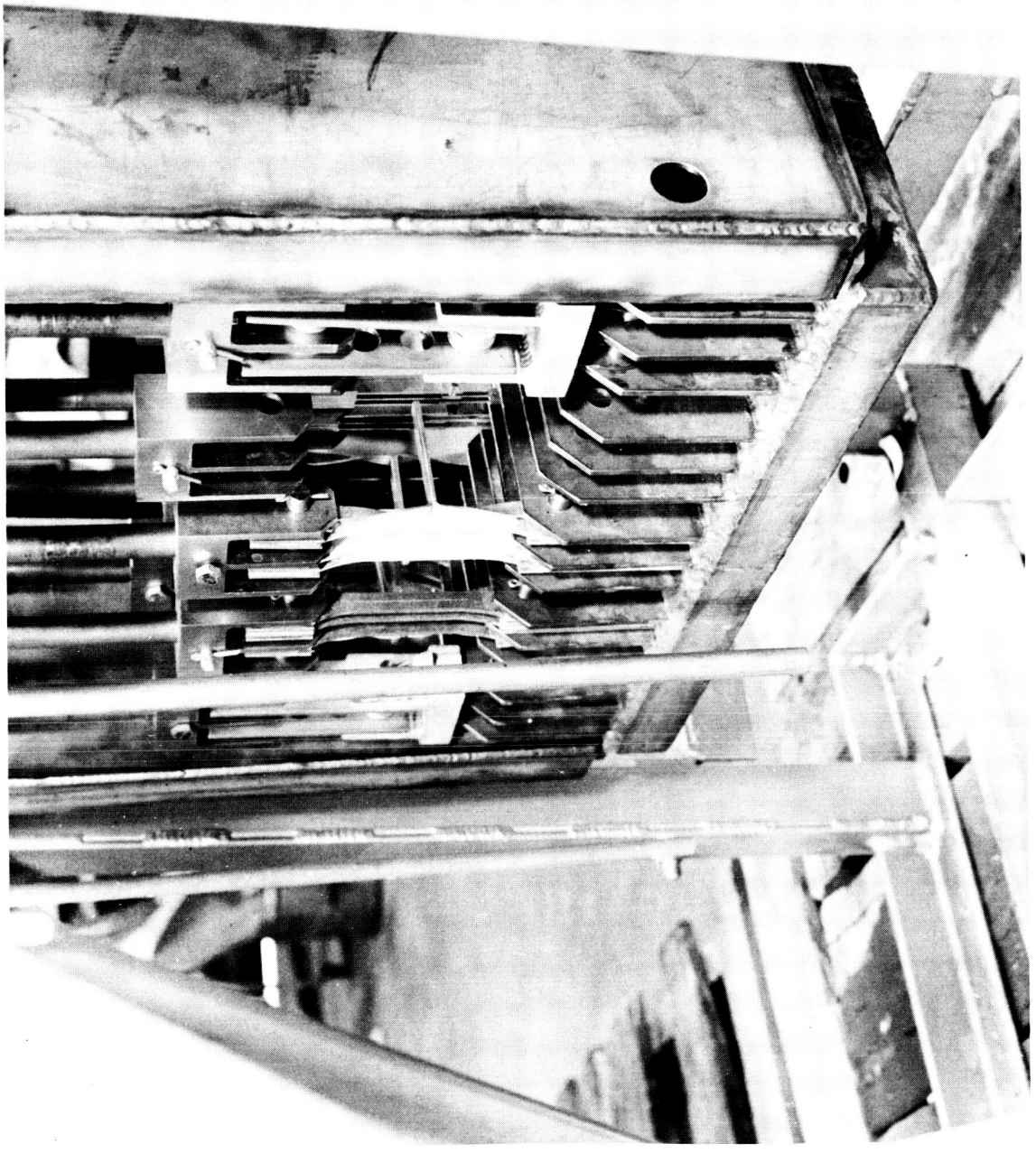

Figure 3.23 Specimen Mounting Arrangement for LN_2 Irradiation: Low Dose, Back Side

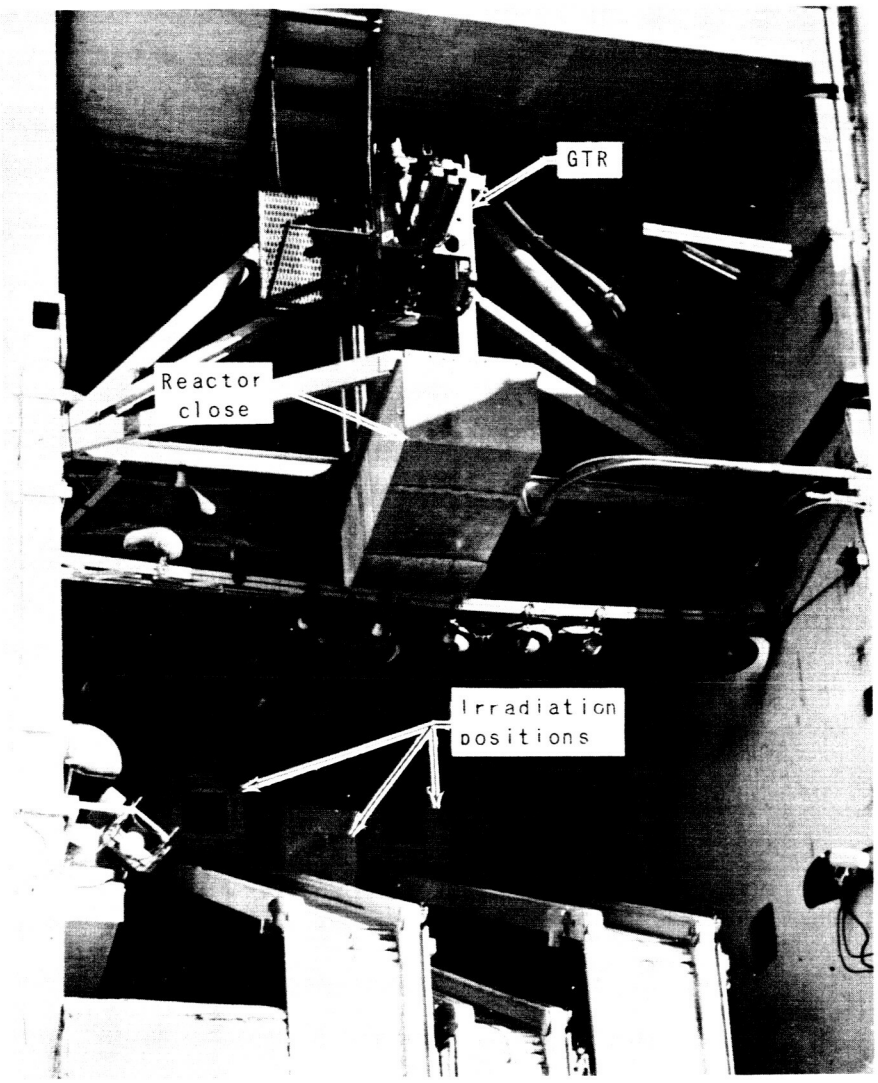

Figure 3.24 Irradiation Pool

NPC 17,793
31-6312

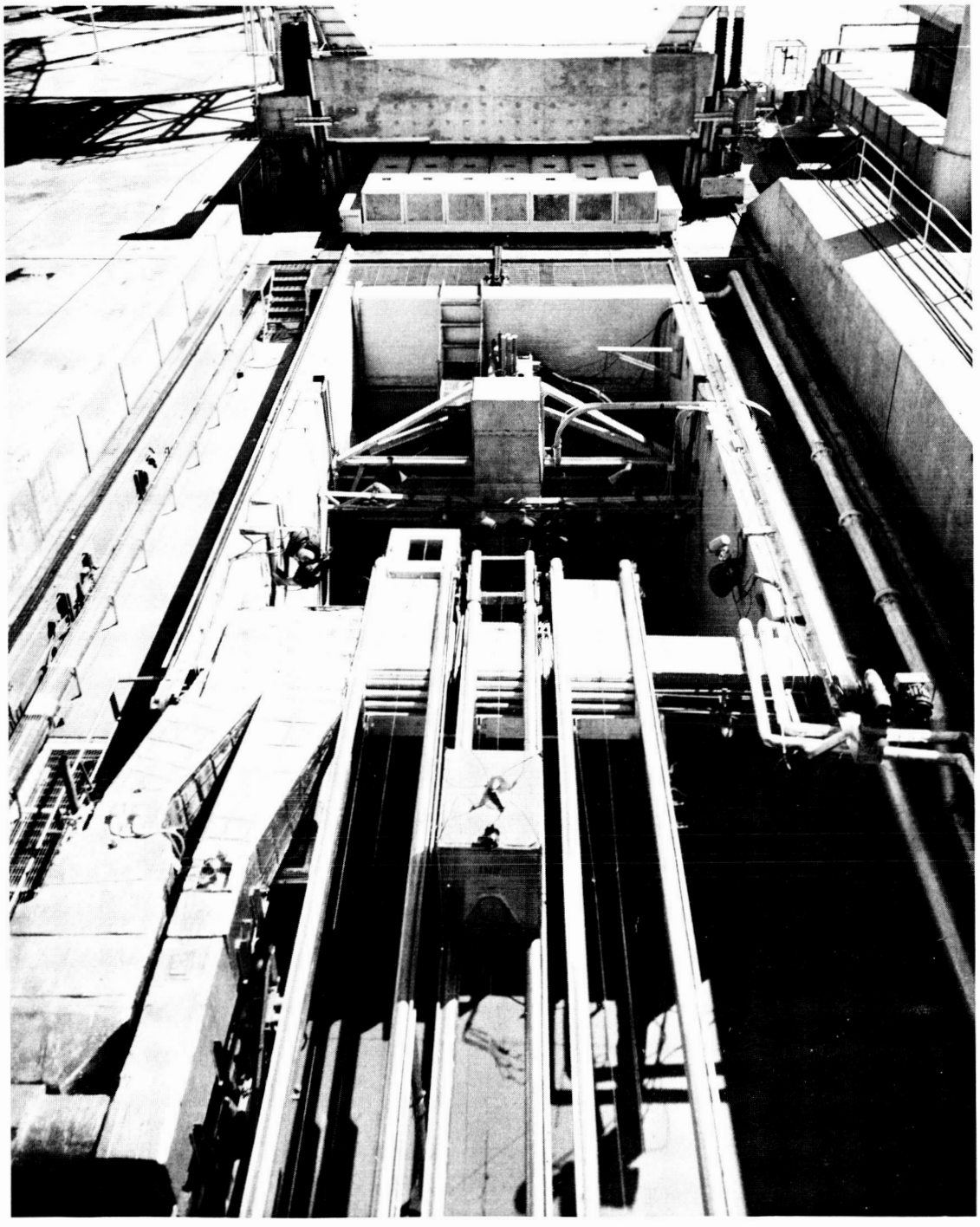

Figure 3.25 Radiation Effects Testing System

NPC 17,794
31-6992

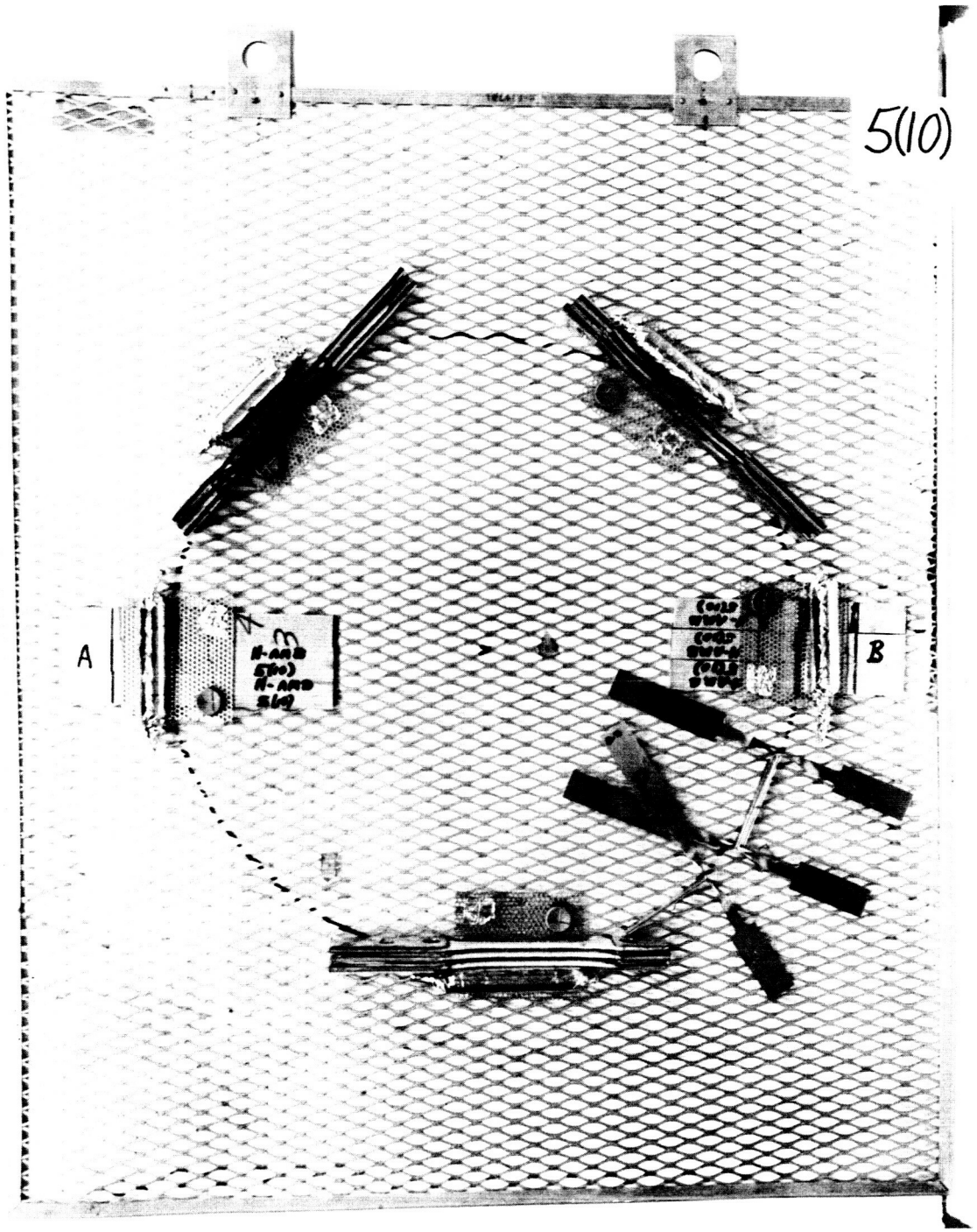

Figure 3.26 Specimen Mounting Arrangement for Ambient-Air Irradiation: High Dose

NPC 17,795
31-6991

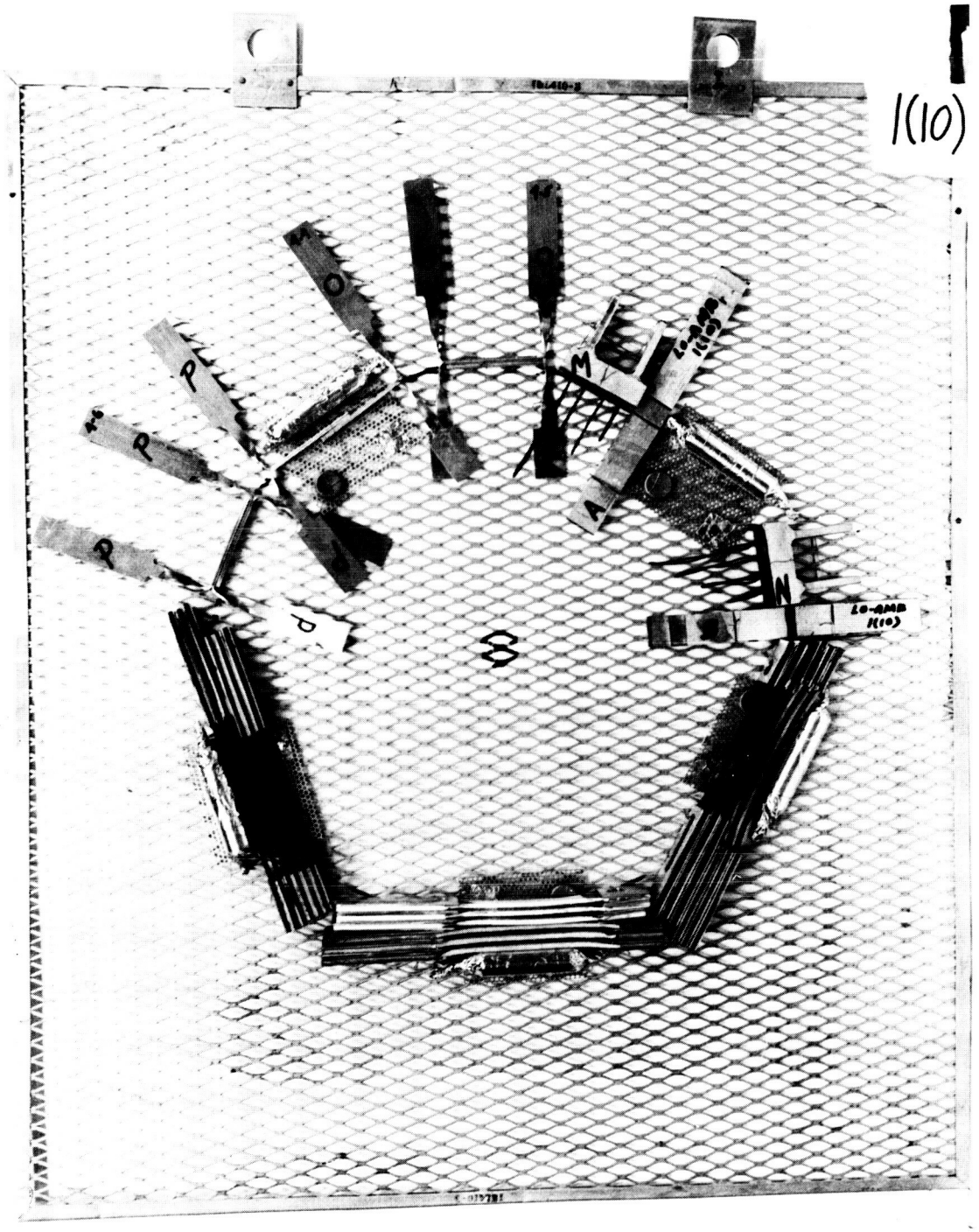

Figure 3.27 Specimen Mounting Arrangement for Ambient-Air Irradiation: Intermediate Dose

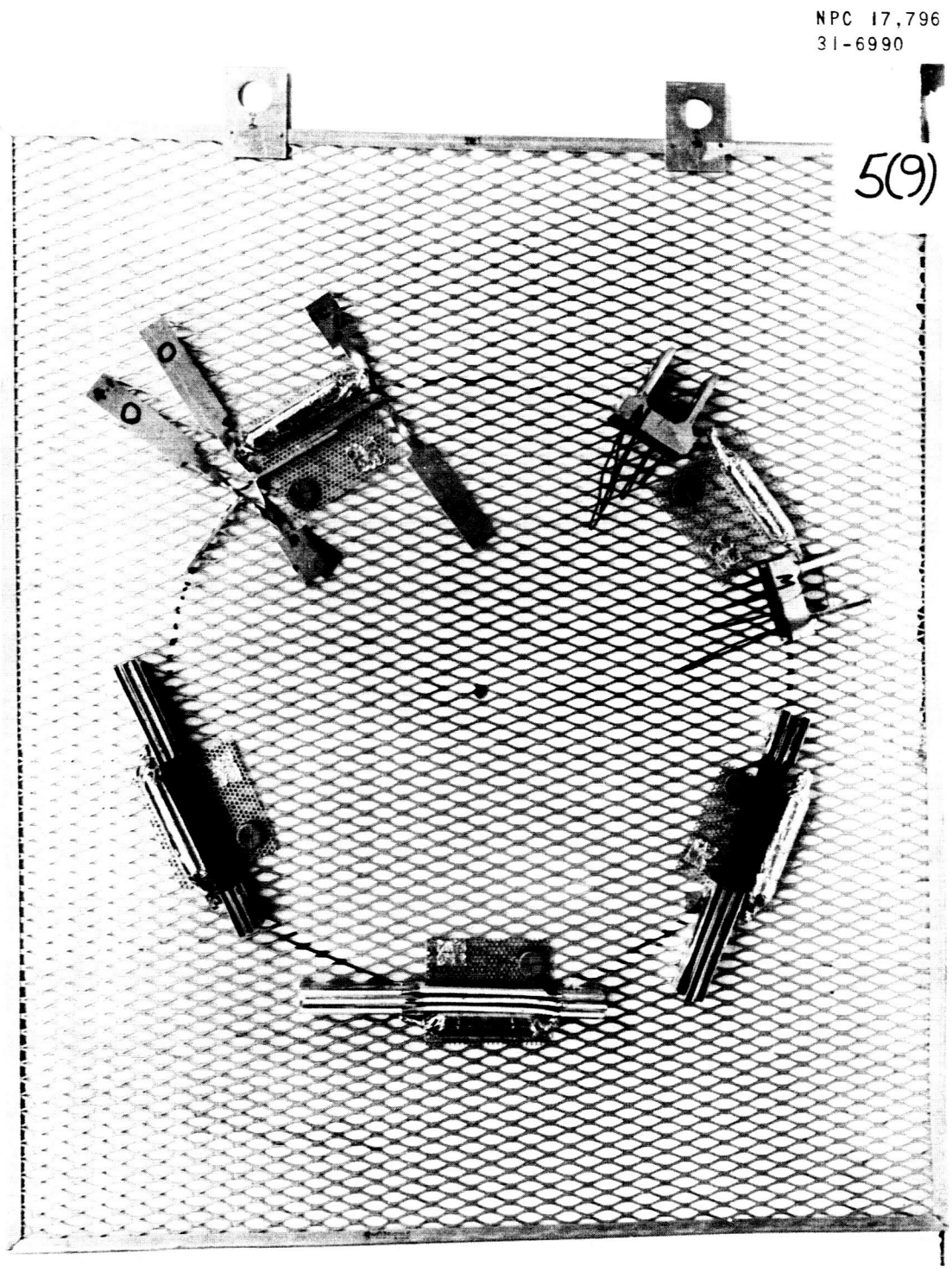

Figure 3.28 Specimen Mounting Arrangement for Ambient-Air Irradiation: Low Dose

Table 3.4

Ambient-Air Irradiation:* North Position

Rack No.	Dose ergs/gm(C)	Dose Rate ergs/gm(C) -hr-3Mw	Length of Irradiation	Distance of Rack from Front of Frame (in.)	Specimen Mounting Radius (in.)
1	5×10^9	1.02×10^9	4.9	10	10
2	1×10^{10}	9.27×10^8	10.8	12	9
3	5×10^{10}	1.513×10^9	33.02	2.25	10

* Four inches of H_2O between reactor core and closet face.

For the low-dose LN_2, irradiation, the west experimental assembly was used and specimens were mounted as shown in Figures 3.22 and 3.23. Details of the specimen layout, gamma doses, and times of irradiation for each material are given in Table 3.5.

3.7 Postirradiation Materials Tests

After each successive period of irradiation during the low-dose LN_2 run, the reactor was shutdown and tensile tests were performed on the appropriate materials, using the Instron machine and interconnecting hydraulic servosystem. The tests were carried out without incident except for the postirradiation ozone detonations described previously in this report.

A description of the tests and data for each material after irradiation to both low and high doses at ambient-air temperature and to a low-dose at LN_2 temperature is presented below:

Adhesives

Material A: AF-40. Irradiation in air to a low dose failed to change the lap-shear strength of this material from about 3000 psi, but, after a high dose, served to reduce the lap-shear strength to 1300 psi. After irradiation to a low dose in LN_2, the lap shear strength at LN_2 temperature was reduced to an average of 1300 psi for the three specimens tested.

Material B: 422J. Data taken from tests on this material demonstrated that it is unaffected by radiation to the prescribed doses, either at ambient-air temperature or at LN_2 temperature.

Seals and Thermal Insulations

Materials C, D, E, F, and G. Comments pertinent to these materials were made previously under Section 3.5.

Table 3.5

Low Dose Liquid-Nitrogen Irradiation Layout: West Dewar

Rod 10	Rod 9	Rod 8	Rod 7	Rod 6
Material N (4) 1.6×10^8 ergs/gm(C)-Hr-Mw 10.4-hr irradiation	- - 1.85×10^8 ergs/gm(C)-hr-Mw - -	Material H (3) Material O (1) 2.1×10^8 ergs/gm(C)-hr-Mw 7.94-hr irradiation	Material I (3) Material O (1) 1.8×10^8 ergs/gm(C)-hr-Mw 9.27-hr irradiation	Material M (4) 1.5×10^8 ergs/gm(C)-hr-Mw 11.1-hr irradiation
Rod 5	**Rod 4**	**Rod 3**	**Rod 2**	**Rod 1**
Material L (3) Material P (1) 3.5×10^8 ergs/gm(C)-hr-Mw 9.5-hr irradiation	Material K (3) Material P (1) 3.55×10^8 ergs/gm(C)-hr-Mw 9.4-hr irradiation	Material A (3) Material B (3) 3.6×10^8 ergs/gm(C)-hr-Mw 9.25-hr irradiation	Material D (3) Material O (1) 3.4×10^8 ergs/gm(C)-hr-Mw 4.9-hr irradiation	Material J (3) Material P (1) 3.2×10^8 ergs/gm(C)-hr-Mw 10.4-hr irradiation

Reactor Side

Electrical Insulations

Material H: Geon 8800. No irradiation data were obtained, either at ambient-air or at LN_2 temperature. All specimens shattered in the doublers prior to tensile tests. Possible changes in doubler design and application are presently being considered.

Material I: Duroid 5600. After irradiation in air to a low dose, the ultimate tensile strength of the material dropped to 1200 psi from the no-irradiation value of 2800 psi; after the specified high dose in air, the ultimate tensile strength dropped to zero. After irradiation to a low dose while submerged in LN_2, subsequent tensile tests (with the material still submerged in the LN_2) revealed an increase in the ultimate tensile from a no-dose value of 4300 psi to a value of 5600 psi. This is a surprising development for Teflon.

Material J: Milimene-Glass 6038. Tests on this material after irradiation in air and in LN_2 revealed that it is virtually unaffected by either the low or high doses of radiation.

Structural Laminates

Material K: CTL-91-LD. Tests on this material after irradiation in air and in LN_2 revealed that it is virtually unaffected by either the low or high doses.

Material L: DC-2104. Tests on this material in air and in LN_2 revealed that it is virtually unaffected by either the low or high doses.

Potting Compounds

Material M: Epon 828/Z. Irradiation and subsequent testing of this material in ambient air revealed that it is virtually unaffected by either a low or high dose at this temperature. Data on tests at LN_2 temperature seem to imply that the break-out force for the wire is higher after a low dose of radiation.

Material N: EC-2273 B/A. Radiation at ambient-air temperature served to reduce the maximum T-peel load by a factor of one-half. The adherents failed to hold to the sealant at LN_2 temperature and no data under this condition were obtained.

Material P: EC-1663. T-peel strength of this material, after irradiation at ambient-air temperature, was only one-sixth of its value before irradiation. The adherents failed to hold to the sealant at LN_2 temperature and no data were obtained under these conditions.

Again this year, as was done with data taken in the first tests under the program in 1962, calculations will be made to determine the extension of a hypothetical 2-in. gage length in dumbbell-type specimens tested in tension in the cryogenic experimental assemblies. Methods for the calculations are shown in Reference 2.

3.8 Statistical Analysis Procedures

A statistical analysis of tensile-shear-strength data taken on lap-shear adhesive specimens will be made. Procedure for this analysis will be as follows:

The experimental design is based on a factorial arrangement of the factors to be investigated. It is for 2 factors each at 3 levels, or 32 treatment combinations. The factors and levels are:

Factors	Levels
Temperature	t_0 - ambient t_1 - LN_2 t_2 - LH_2
Radiation	d_0 - 0 dose d_1 - low dose d_2 - high dose

The 9 treatment combinations are:

Radiation	Temperature		
	t_0	t_1	t_2
d_0	1	2	3
d_1	4	5	6
d_2	7	8	9

The number of treatment combinations to be investigated is larger than can be carried out under uniform conditions of one homogeneous group of lap-shear sheets. There are 13 lap-shear sheets with 5 specimens available per sheet. Therefore, a design is required which will divide the experimental resources in such a manner that the estimates of the main effects and interactions can be obtained free from the possible differences between the sheets.

There are factorial designs in which confounding can be used to obtain estimates free of the sheet differences, but in this case it is simpler and more straightforward to obtain separate estimates of the sheet differences from a "side" experiment and to adjust the data from the main experiment accordingly. The main experiment will use 3 specimens from each of 9 sheets and the remaining 2 specimens will be used in the "side" experiment for estimating the sheet differences.

The procedure is as follows: Let the sheets be A, B, C, D, E, F, G, H, and K and the samples from each sheet be a_1, a_2, ---, a_5 for Sheet A, b_1, ---, b_2 for Sheet B and so on. The samples are allotted to the experimental treatment as:

1 - adga*	2 - aeh	3 - afk
4 - bdk	5 - beg	6 - bfh
7 - cdh	8 - cek	9 - cfg

* Four samples in this treatment, $d_o t_o$.

The two remaining samples per sheet will be tested in the experimental assemblies under ambient conditions for estimating the sheet differences.

The data from the main experiment will be adjusted according to the estimates of the sheet differences obtained in the "side" experiment. This adjustment will essentially normalize the data to an overall sheet average, so that the resulting data can be analyzed as a 3^2 factorial by an analysis of variance method. One will then be able to obtain estimates of the effects of:

Liquid Temperature
Quadratic Temperature
Linear Radiation
Quadratic Radiation
Interaction of Temperature and Radiation

The main disadvantage of the design stems from the fact that there will be no valid estimate of the experimental error for assessing whether the observed differences from

one treatment to another are real effects or just change occurrences. This is not a consequence of the design but of non-replication of the basic experiment, because even if there were 100 samples exactly alike there still would not be a valid estimate of the experimental error (the ability or inability to reproduce the experimental setup on independent trails of the basic experiment).

IV. COMBINED EFFECTS OF RADIATION, VACUUM, AND CRYOTEMPERATURES

A program has been initiated to evaluate the combined effects of radiation, vacuum, and cryotemperature on selected materials. In order to perform these tests at cryotemperatures in vacuum immediately after irradiation, two special testers are being built: an Electrical Tester to measure dielectric and dissipation factor and a Mechanical Tester to measure stress-strain properties.

4.1 Test-Material Selection

The selection of the candidate materials for these tests was based on the results of the vacuum-radiation tests and the cryotemperature-radiation tests presented in the two-volume annual report (Refs. 1, 2), and from the tests performed during April. Table 4.1 identifies the materials being considered for evaluation during this program. These materials will be evaluated in the dynamic testers to establish control values before final selection is made for the irradiation test.

4.2 Test Equipment

The Electrical Testing is being designed and constructed by NASA at the George C. Marshall Space Flight Center under the direction of R. L. Gause. Operational checkout of the system is scheduled for the middle of June.

Table 4.1

Materials and Suggested Test for
Vacuum-Cryogenic-Irradiation Experiment

Category	Chemical Class	Trade Name	Suggested Test
Dielectric Materials	Fluoroethylene	Teflon TFE	Dielectic
	Fluoroethylene	Teflon FEP	Dielectric and Tensile
	Polyimid	SP Plastic	Tensile
	Polyethylene	Marlex 6002	Dielectric and Tensile
	Polyolofin	Thermofit	Dielectric
Electrical Insulations	Polyvinyl chloride	Geon 8800	Dielectric and Tensile
	Polyvinyl chloride	Estane 5740	Dielectric
Potting Compounds	Epoxy Resin	Scotchcast 212	Dielectric
	Epoxy Resin	Epon 828/Z	Dielectric
	Silicone	RTV-60	Dielectric

The tester is designed to fit into the vacuum-irradiation chambers, with the cryogen contained in a shroud that fits into the vacuum chamber and around eight dielectric test cells. The test cells, being in vacuum, will be cooled by radiant and conductive heat transfer only, for the cells are not to be immersed in the cryogenic fluid. The eight test cells are designed in accordance with ASTM D-150-54T ("A. C. Capacitance, Dielectric Constant, and Loss Characteristics of Electrical Insulating Material"), which calls for a test specimen to be 4 in. in diameter and 1/8 in. thick.

The Mechanical Tester is designed to fit into the vacuum-irradiation chambers and to test the mechanical properties of materials in tension. Liquid hydrogen will be contained in tubes coiled around the test samples rather than in a shroud, as previously considered. A minimum of structural material will be used in the tester to minimize gamma-heating; however, for 5000 -lb load capability, a considerable quantity of structural material has to be used. This means that the sample temperature will be above the boiling point of the liquid-hydrogen cryogen.

The hydraulic pulling mechanism and load-weighing system is patterned after the High-Force Tensile Tester. This tester is designed with interchangeable load cell for a maximum load range of 5000 lb, but it still gives good sensitivity ($\pm$ 1 lb) for the low-load ranges. Five pull-rod positions are available to pull the standard ASTM test specimen.

4.3 Test Plan

Candidate test materials listed in Table 4.1 will be tested at cryogenic temperatures prior to the irradiation test to establish control values. From these data, the materials for irradiation will be selected.

Dielectric measurements will be made at predetermined intervals during the irradiation. During these measurements, the reactor will be retracted (zero effective dose rate) so that the temperature of the sampler will have time to stabilize at the cryogenic fluid temperature before the measurements are recorded. Several measurements will also be taken while the reactor is at power.

Tensile tests will be made at the end of the irradiation while the samples are still in vacuum and at cryotemperature. The measured properties will be modulus, ultimate tensile strength, and ultimate elongation.

REFERENCES

1. Kerlin, E. E., Investigation of Combined Effects of Radiation and Vacuum and of Radiation and Cryotemperatures on Engineering Materials. Volume I: Radiation Vacuum Test. Annual Report 9 November 1961 through 8 November 1962. General Dynamics/Fort Worth Report FZK-161-1 (5 January 1963). U

2. Smith, E. T., Investigation of Combined Effects of Radiation and Vacuum and of Radiation and Cryotemperatures on Engineering Materials. Volume II: Radiation-Cryotemperature Test. Annual Report, 9 November 1961 through 8 November 1962. General Dynamics/Fort Worth Report FZK-161-2 (5 January 1963). U

3. Kerlin, E. E., and Smith, E. T., Measured Effects of the Various Combinations of Nuclear Radiation, Vacuum, and Cryotemperatures on Engineering Materials. Quarterly Progress Report, 9 November 1962 through 28 February 1963. General Dynamics/Fort Worth Report FZK-163 (15 March 1963).

4. Bochirol, L., Doulat, J., and Weil, L., "Principle of a Liquid-Nitrogen Irradiation Device and Its Realization for Use in a Swimming-Pool-Type Reactor." Advances in Cryogenic Engineering, edited by K. D. Timmerhaus. New York: Plenum Press, Inc. (1961), Vol. 6, pp. 130-135 (Paper No. B-7). Proceedings of the 1960 Cryogenic Engineering Conference, University of Colorado and National Bureau of Standards, Boulder, Colo., August 23-25, 1960.

5. Thorp, C. E., "Decomposition and Explosion Limits." Physical and Pharmacological Properties. Part I: Physical Properties. Chicago: Armour Research Foundation of Illinois Institute of Technology, Vol. 2, Chap. XI, pp. 30-41.

6. Freeman, B. F., and Fleming, F. F., Experimental Mapping of the Irradiation Volumes of the Convair Radiation Effects Testing Facility. Convair-Fort Worth Report MR-N-262 (NARF-60-30T, 30 November 1960.

DISTRIBUTION LIST

ADDRESSEE	NO. OF COPIES
National Aeronautics and Space Administration George C. Marshall Space Flight Center Huntsville, Alabama Attn: M-P and C-CA	12
National Aeronautics and Space Administration Langley Research Center Langley Field, Virginia	1
National Aeronautics and Space Administration Manned Spacecraft Center Houston, Texas	1
National Aeronautics and Space Administration Ames Research Center Moffett Field, California	1
Bernard Ackhammer National Aeronautics and Space Administration Washington 25, D. C.	1
Robert Brock National Aeronautics and Space Administration Rich Building - Room 271 6040 Telephone Road Houston, Texas	1
SNPO-Cleveland Lewis Research Center 21000 Brookpark Road Cleveland 35, Ohio	1
Mort Krasner Reactor Division Lewis Research Center 21000 Brookpark Road Cleveland 35, Ohio	1
Dr. Henry Frankel Goddard Space Flight Center Greenbelt, Maryland	1
Dan Reigert National Aeronautics and Space Administration Instrument and Electronic Systems Division Rich Building 6040 Telephone Road Houston, Texas	1

DISTRIBUTION LIST (Cont'd)

ADDRESSEE	NO. OF COPIES
J. H. Kimzey Mechanical Systems Branch SEDD National Aeronautics and Space Administration 6040 Telephone Road Houston, Texas	1
Capt. Harold E. Pilcher Headquarters SSD (SSZMS) AF Unit Post Office Los Angeles 45, California	
Scientific and Technical Information Facility Post Office Box 5700 Bethesda, Maryland Attn: NASA Representative (S-AK/RKT)	2
John Morrissey Space Nuclear Propulsion Office Division of Reactor Development U. S. Atomic Energy Commission Germantown, Maryland	1
Oscar Sisman Solid State Division Oak Ridge National Laboratory Oak Ridge, Tennessee	1
Plastics Technical Evaluation Center Picatinny Arsenal Dover, New Jersey Attn: H. E. Pebly	2
R. W. Bowman Radiation Effects Information Center Battelle Memorial Institute 505 King Avenue Columbus 1, Ohio	1
John B. Rittenhouse Lockheed Missiles and Space Company Research Laboratories, 52-30 3251 Hanover Street Palo Alto, California	1
Dr. F. J. Clauss Lockheed Missiles and Space Company Palo Alto, California	1

DISTRIBUTION LIST (Cont'd)

ADDRESSEE	NO. OF COPIES
D. M. Newell Dept. 52-10, Bldg. 204 Lockheed Missiles and Space Company Palo Alto, California	1
Oliver Burford Lockheed Georgia Company Marietta, Georgia	1
Dr. Hand Plank Lockheed Missiles and Space Company Sunnyvale, California	1
Dr. George Yasui Dept. 3202, Bldg. 537 Lockheed Missiles and Space Company Sunnyvale, California	1
L. D. Jaffee Jet Propulsion Laboratory 4800 Oak Grove Drive Pasadena 3, California	1
Robert Harrington Jet Propulsion Laboratory 4800 Oak Grove Drive Pasadena 3, California	1
William F. Emmons Dept. 746, Bldg. 160 Aerojet General Corporation Azusa, California	1
P. H. Sager GD/Astronautics San Diego, California	1
S. A. Yalof GD/Astronautics San Diego, California	1
AVCO Corporation Spaceflight Program Office 6501 E. Admiral Place Tulsa 15, Oklahoma Attn: M. I. Gamble	1